Keyhole Effect in Dual-Hop MIMO AF Relay Transmission with Space-Time Block Codes

Trung Q. Duong, *Student Member, IEEE*, Himal A. Suraweera, *Member, IEEE*, Theodoros A. Tsiftsis, *Senior Member, IEEE*, Hans-Jürgen Zepernick, *Senior Member, IEEE*, and Arumugam Nallanathan, *Senior Member, IEEE*

***Abstract*—In this paper, the effect of keyhole on the performance of multiple-input multiple-output (MIMO) amplify-and-forward (AF) relay networks with orthogonal space-time block codes (OSTBCs) transmission is investigated. In particular, we analyze the asymptotic symbol error probability (SEP) performance of a downlink communication system where the amplifying processing at the relay can be implemented by either the linear or squaring approach. Our tractable asymptotic SEP expressions enable us to obtain both diversity and array gains. Our finding reveals that with condition $n_{\mathsf{S}} > \min(n_{\mathsf{R}}, n_{\mathsf{D}})$, the linear approach can provide the full achievable diversity gain of $\min(n_{\mathsf{R}}, n_{\mathsf{D}})$ when only the second hop suffers from the keyhole effect, i.e., single keyhole effect (SKE), where n_{S}, n_{R}, and n_{D} are the number of antennas at source, relay, and destination, respectively. However, for the case that both the source-relay and relay-destination links experience the keyhole effect, i.e., double keyhole effect (DKE), the achievable diversity order is only one regardless of the number of antennas. In contrast, utilizing the squaring approach, the overall diversity gain can be achieved as $\min(n_{\mathsf{R}}, n_{\mathsf{D}})$ for both SKE and DKE. An important observation corroborated by our studies is that for satisfying the tradeoff between performance and complexity, we should use the linear approach for SKE and the squaring approach for DKE.**

***Index Terms*—Keyhole effect, amplify-and-forward relay, multiple-input multiple-output, orthogonal space-time block code.**

I. Introduction

THE multiple-input multiple-output (MIMO) technique has been considered as a promising transmission scheme for future wireless systems as being included in the extension of the 3GPP Long Term Evolution (LTE) standard. By deploying multiple antennas at transmitter and receiver ends, MIMO systems exploit the rich scattering propagation environment of wireless links to enhance the system performance [1]. In this ideal case of rich scattering, the channel matrix is of full rank. As a consequence, a MIMO channel between an n_{S}-antenna source and an n_{D}-antenna destination under such ideal condition exhibits the maximum multiplexing gain of $\min(n_{\mathsf{S}}, n_{\mathsf{D}})$ and diversity gain of $n_{\mathsf{S}} n_{\mathsf{D}}$. In some realistic indoor and outdoor propagation conditions such as corridors, crowded subways and tunnels, scattering objects can be randomly arranged, which may cause a rank deficiency of the channel matrix. This degeneration effect, so called keyhole or pinhole effect, significantly decreases the spatial multiplexing and diversity gains in MIMO systems [2]–[4]. As a result, the keyhole effect reduces the MIMO channel capacity to that of single-input single-output (SISO) systems and the diversity gain is of $\min(n_{\mathsf{S}}, n_{\mathsf{D}})$ order.

MIMO relay networks have attracted much interest because of their ability to remarkably increase coverage and system performance [5], [6]. However, there has been limited research in the contemporary literature investigating the keyhole effect on the performance of MIMO relay networks. To the best of the authors' knowledge, only Souihli and Ohtsuki have very recently attempted to consider the effect of keyhole for MIMO relay systems [7], [8]. In particular, by considering a downlink cellular network in which the source-to-relay channel enjoys rich scattering while the source-to-destination and relay-to-destination channels suffer from the keyhole phenomenon, they have shown that using the relay can mitigate the effect of the keyhole in terms of channel capacity. However, [7] and [8] have only focused on the multiplexing gain and the decode-and-forward (DF) relay protocol. In our previous work [9], we have investigated the cooperative diversity gain for a similar downlink system with orthogonal space-time block code (OSTBC) transmission. We have shown that the antenna correlation has no impact on the diversity gain of MIMO keyhole relay channels.

The OSTBC transmission over MIMO amplify-and-forward (AF) relay networks can be subdivided into two groups depending on the signal processing at the relay: 1) *Linear Approach*: the relay simply amplifies the source's OSTBC matrix and forwards it to the destination without incurring any additional processing [10], [11] and 2) *Squaring Approach*: the relay performs the squaring technique [12] to decompose the source's OSTBC matrix into independent SISO signals and then re-encodes them by a new OSTBC matrix before forwarding to the destination [13]–[15]. It is important to note that for the linear approach, the relay can operate in either semi-blind or channel state information (CSI)-assisted modes. However, for the squaring approach, since the relay utilizes the CSI knowledge for decoupling the source's OSTBC matrix, it is reasonable to assume that the AF relay will operate using the CSI-assisted gain.

Several papers have investigated the performance of OSTBCs in AF relay systems (see e.g., [10], [11], [13]–[15]

Paper approved by N. Al-Dhahir, the Editor for Space-Time, OFDM and Equalization of the IEEE Communications Society. Manuscript received September 14, 2011; revised April 6 and July 11, 2012.

T. Q. Duong and H.-J. Zepernick are with the Blekinge Institute of Technology, Sweden (e-mail: {quang.trung.duong, hans-jurgen.zepernick}@bth.se).

H. A. Suraweera is with the Singapore University of Technology and Design, Singapore (e-mail: himalsuraweera@sutd.edu.sg).

T. A. Tsiftsis is with the Technological Educational Institute of Lamia, Greece (e-mail: tsiftsis@teilam.gr).

A. Nallanathan is with the King's College London, United Kingdom (e-mail: arumugam.nallanathan@kcl.ac.uk).

Digital Object Identifier 10.1109/TCOMM.2012.110616.110616

and references therein). For the linear approach, the exact symbol error probability (SEP) for semi-blind AF relay has been derived for dual-hop fading channel in [10]. The final SEP expression in [10] is not given in closed-form expression but as an integral whose integrand is expressed in terms of hypergeometric functions. In [11], several closed-form expressions of the bit error rate (BER) for a specific number of antennas have been presented. For the squaring approach, the error rate performance has been investigated for the cases when the destination has a single antenna [14] and multiple antennas [13]. The performance of OSBTC transmission in MIMO AF relay networks with best relay selection has been addressed in [15].

In this paper, we investigate the effect of MIMO keyhole channels on the cooperative diversity gain of relay networks. We consider the downlink cooperative communication where an n_{S}-antenna base station S using OSTBC communicates with an n_{D}-antenna mobile station D through the assistance of an n_{R}-antenna relay station R. To distinguish the advantage of each type of signal processing at R, the linear approach is assumed to operate in semi-blind mode for low complexity processing while in the squaring approach the CSI-assisted AF relay is exploited to perform some additional complicated processing. In addition, we consider both single keyhole effect (SKE) and double keyhole effect[1] (DKE). For the case of SKE, the relay is assumed to be a fixed base station (BS) and placed in some strategic location, leading the source-to-relay link to enjoy rich scattering whereas the relay-to-destination link suffers poor scattering due to the mobility of the destination. For the case of DKE, due to ad-hoc relay placement or in some specific networks such as vehicle-to-vehicle communication [16], [17], we assume that both hops are subject to the keyhole effect.

Our contributions include the following:

- We develop new analytical expressions to investigate the performance of AF systems with OSTBCs and keyhole effects for downlink communication[2]. In particular, we investigate the system's average SEP for both linear and squaring approaches.
- We present new asymptotic results which reveal the effect of keyhole on diversity and array gains of the considered system for both linear and squaring approaches. For SKE, the relaying channel (source-relay-destination link) provides the full cooperative diversity gain of $\min(n_{\mathsf{R}}, n_{\mathsf{D}})$ for both AF relaying approaches (linear and squaring). However, for the case of DKE, the linear approach cannot offer any diversity gain, i.e., its diversity order is equal to that of a SISO channel. In contrast, for the squaring approach, the full achievable diversity gain remains as $\min(n_{\mathsf{R}}, n_{\mathsf{D}})$.
- Our analysis gives additional insights for the system designer that for keyhole relay channels, the deployment of more than n_{D} antennas at the relay, i.e., $n_{\mathsf{R}} > n_{\mathsf{D}}$, yields no diversity gain. More importantly, when only the second hop suffers from the keyhole effect, the relay should deploy the linear approach to achieve the full diversity gain with low complexity. When both hops experience the keyhole effect, the squaring approach is more favorable than the linear approach because it can only offer a unit diversity order.

[1]In referring here to SKE, we imply that the first hop is assumed to be keyhole-free and subject to Rayleigh fading. In contrast, for DKE both hops experience the keyhole effect. For a single-antenna relay system, the keyhole channel for mobile relay particularizes to a double fading channel [16], [17].

[2]In this paper, we have assumed that $n_{\mathsf{S}} > \min(n_{\mathsf{R}}, n_{\mathsf{D}})$ for all cases. Since the considered system is downlink, i.e., $n_{\mathsf{S}} > n_{\mathsf{D}}$, the above condition is always satisfied. As a result, downlink communication implicitly indicates that $n_{\mathsf{S}} > \min(n_{\mathsf{R}}, n_{\mathsf{D}})$.

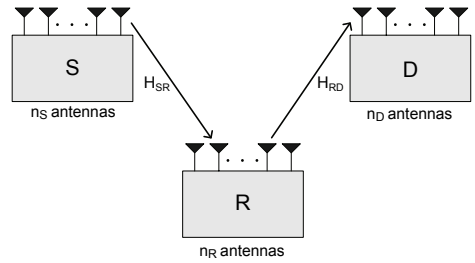

Fig. 1. System model for a dual-hop MIMO AF relay system consisting of an n_{S}-antenna source, an n_{R}-antenna relay, and an n_{D}-antenna destination. (a) SKE: $\boldsymbol{H}_{\mathrm{RD}}$ is subject to the keyhole effect and $\boldsymbol{H}_{\mathrm{SR}}$ is keyhole-free. (b) DKE: Both $\boldsymbol{H}_{\mathrm{SR}}$ and $\boldsymbol{H}_{\mathrm{RD}}$ are subject to the keyhole effect.

Notation: Vectors and matrices are written as bold lowercase and uppercase letters, respectively. Superscripts $*$ and $\dagger$ stand for complex conjugate and transpose conjugate, respectively. $\boldsymbol{I}_n$ represents an $n \times n$ identity matrix and $\|\boldsymbol{A}\|_{\mathrm{F}}$ defines Frobenius norm of the matrix $\boldsymbol{A}$. $\mathbb{E}\{.\}$ and $\mathrm{tr}(\cdot)$ are the expectation operator and trace of a matrix, respectively. We use the notation $x \sim \mathcal{CN}(\cdot,\cdot)$ to denote that x is complex circularly symmetric Gaussian distributed. Let $\boldsymbol{x} \in \mathbb{C}^m$ be the complex Gaussian distributed vector-variate with mean vector $\boldsymbol{v}$ and variance matrix $\boldsymbol{\Sigma}$ defined as $\boldsymbol{x} \sim \tilde{\mathcal{N}}_m(\boldsymbol{v}, \boldsymbol{\Sigma})$. $\mathcal{K}_\nu(\cdot)$ is the modified Bessel function of the second kind [18, Eq. (8.432.3)]. Finally, let $\boldsymbol{X} \in \mathbb{C}^{m\times n}$ be the complex Gaussian distributed matrix-variate defined as $\boldsymbol{X} \sim \tilde{\mathcal{N}}_{m,n}(\boldsymbol{M}, \boldsymbol{\Sigma}, \boldsymbol{\Phi})$ if $\mathrm{vec}(\boldsymbol{X}^\dagger)$ is mn-variate complex Gaussian distributed with mean $\mathrm{vec}(\boldsymbol{M}^\dagger)$ and covariance $\boldsymbol{\Sigma}^T \otimes \boldsymbol{\Phi}$, where $\otimes$ is the Kronecker product and $\mathrm{vec}(\boldsymbol{A})$ denotes the vector formed by stacking all the columns of $\boldsymbol{A}$ into a column vector.

II. System and Channel Models

We consider a communication network where a source terminal S communicates with a destination D through the assistance of a relay station R as shown in Fig. 1. In this paper, we assume no direct link between the source and destination due to high pathloss and severe shadowing.

We next describe OSTBC transmission over a dual-hop AF relay network in detail. During an L_c-symbol interval, $N \log_2 M$ information bits are mapped to a sequence of symbols $x_1, x_2, ..., x_N$ selected from an M-ary phase-shift keying (M-PSK) or M-ary quadrature amplitude modulation (M-QAM) signal constellation $\mathcal{S}$ using Gray mapping with average transmit energy per symbol $\mathbb{E}\{|x_k|^2\} = P_0$. These symbols are then encoded with an OSTBC denoted by an $L_c \times n_{\mathsf{S}}$ transmission matrix $\boldsymbol{\mathcal{G}}$ with code rate $\mathcal{R}_c$ whose elements are the linear combinations of $x_1, x_2, ..., x_N$ and their conjugate with the property that the columns of $\boldsymbol{\mathcal{G}}$ are orthogonal [19].

We assume that the channel is subject to frequency-flat fading and is perfectly known at the destination but unknown

at the source. The source will transmit the OSTBC matrix $\boldsymbol{X} = \boldsymbol{\mathcal{G}}^T$ to the relay in the first hop. Let us denote P_s as the transmit power in n_{S} antennas at the source so that the total transmit power of an OSTBC block is $\mathbb{E}\left\{\|\boldsymbol{X}\|_{\mathrm{F}}^2\right\} = L_c P_s$. The signal received at the relay in the first hop is given by $\boldsymbol{Y}_{\mathrm{SR}} = \boldsymbol{H}_{\mathrm{SR}}\boldsymbol{X} + \boldsymbol{W}_{\mathrm{SR}}$, where $\boldsymbol{H}_{\mathrm{SR}} \sim \tilde{\mathcal{N}}_{n_{\mathsf{R}},n_{\mathsf{S}}}(\boldsymbol{0}, \Omega_1 \boldsymbol{I}_{n_{\mathsf{R}}}, \boldsymbol{I}_{n_{\mathsf{S}}})$ is a random channel matrix, with $\Omega_1 = \mathbb{E}\left\{|\{\boldsymbol{H}_{\mathrm{SR}}\}_{ij}|^2\right\}$ for $i = 1, 2, \ldots, n_{\mathsf{R}}$ and $j = 1, 2, \ldots, n_{\mathsf{S}}$, and $\boldsymbol{W}_{\mathrm{SR}} \sim \tilde{\mathcal{N}}_{n_{\mathsf{R}},N_c}(\boldsymbol{0}, N_0 \boldsymbol{I}_{n_{\mathsf{R}}}, \boldsymbol{I}_{L_c})$ is an additive white Gaussian noise (AWGN) matrix, with $N_0 = \mathbb{E}\left\{|\{\boldsymbol{W}_{\mathrm{SR}}\}_{ij}|^2\right\}$.

A. Linear Approach

The received signal at the relay, $\boldsymbol{Y}_{\mathrm{SR}}$, is then multiplied by a fixed gain G_{LA}, and retransmitted to the destination. The signal at the destination in the second hop is given by $\boldsymbol{Y}_{\mathrm{RD}} = \boldsymbol{H}_{\mathrm{RD}} G_{\mathsf{LA}} \boldsymbol{Y}_{\mathrm{SR}} + \boldsymbol{W}_{\mathrm{RD}}$, where $\boldsymbol{H}_{\mathrm{RD}} \sim \tilde{\mathcal{N}}_{n_{\mathsf{D}},n_{\mathsf{R}}}(\boldsymbol{0}, \Omega_2 \boldsymbol{I}_{n_{\mathsf{D}}}, \boldsymbol{I}_{n_{\mathsf{R}}})$ is a random channel matrix, with $\Omega_2 = \mathbb{E}\left\{|\{\boldsymbol{H}_{\mathrm{RD}}\}_{k\ell}|^2\right\}$ for $k = 1, 2, \ldots, n_{\mathsf{D}}$ and $\ell = 1, 2, \ldots, n_{\mathsf{R}}$, and $\boldsymbol{W}_{\mathrm{RD}} \sim \tilde{\mathcal{N}}_{n_{\mathsf{D}},L_c}(\boldsymbol{0}, N_0 \boldsymbol{I}_{n_{\mathsf{D}}}, \boldsymbol{I}_{L_c})$ is an AWGN matrix, with $N_0 = \mathbb{E}\left\{|\{\boldsymbol{W}_{\mathrm{RD}}\}_{k\ell}|^2\right\}$.

Utilizing the orthogonal property of OSTBCs, the maximum likelihood (ML) decoding metric can be decomposed into a sum of N terms, where each term depends exactly on one complex symbol $x_n, n = 1, 2, ..., N$. Consequently, the detection of x_n is decoupled from the detection of x_p for $n \neq p$ and the end-to-end instantaneous SNR can be written as [10]

$$\gamma_{\mathsf{LA}} = \frac{\bar{\gamma}}{\mathcal{R}_c n_{\mathsf{S}}} \operatorname{tr}\left\{\left[G_{\mathsf{LA}}^2 \boldsymbol{H}_{\mathrm{RD}}^{\dagger}\left(\boldsymbol{I}_{n_{\mathsf{D}}} + G_{\mathsf{LA}}^2 \boldsymbol{H}_{\mathrm{RD}} \boldsymbol{H}_{\mathrm{RD}}^{\dagger}\right)^{-1} \times \boldsymbol{H}_{\mathrm{RD}} \boldsymbol{H}_{\mathrm{SR}} \boldsymbol{H}_{\mathrm{SR}}^{\dagger}\right]\right\}, \tag{1}$$

where $\bar{\gamma} = P_s/N_0$ is the average SNR and (1) is obtained from the fact that $\mathbb{E}\left\{\|\boldsymbol{X}\|_{\mathrm{F}}^2\right\} = L_c P_s$. Given the condition that the relay does not have full channel knowledge of the first hop, G_{LA} can be obtained as $G_{\mathsf{LA}}^2 = [n_{\mathsf{R}}(\Omega_1 + 1/\bar{\gamma})]^{-1}$ [10], [11]. When the relay is deployed with a single antenna, i.e., $n_{\mathsf{R}} = 1$, the channel matrices $\boldsymbol{H}_{\mathrm{SR}}$ and $\boldsymbol{H}_{\mathrm{RD}}$ for both hops become vectors $\boldsymbol{h}_{\mathrm{SR}}$ and $\boldsymbol{h}_{\mathrm{RD}}$, respectively. The instantaneous SNR for the linear approach given in (1) can now be simplified as

$$\gamma_{\mathsf{LA}} = \frac{\bar{\gamma}}{\mathcal{R}_c n_{\mathsf{S}}} \frac{\|\boldsymbol{h}_{\mathrm{SR}}\|_{\mathrm{F}}^2 \|\boldsymbol{h}_{\mathrm{RD}}\|_{\mathrm{F}}^2}{\|\boldsymbol{h}_{\mathrm{RD}}\|_{\mathrm{F}}^2 + 1/G_{\mathsf{LA}}^2}. \tag{2}$$

B. Squaring Approach

Using the squaring approach [12]–[15] of OSTBC transmission, the received matrix at the relay can be decomposed as $y_k = \|\boldsymbol{H}_{\mathrm{SR}}\|_{\mathrm{F}}^2 x_k + \eta_k$, where $k = 1, 2, \ldots, N$ and $\eta_k \sim \mathcal{CN}\left(0, \|\boldsymbol{H}_{\mathrm{SR}}\|_{\mathrm{F}}^2 N_0\right)$. With the decomposed symbols y_k at hand, the relay generates an OSTBC matrix and then amplifies it with an amplifying gain G_{SA} before transmitting to the destination. For the squaring approach, it is plausible to assume that the relay operates in the CSI-assisted mode and its amplifying gain is defined as $G_{\mathsf{SA}} = (\|\boldsymbol{H}_{\mathrm{SR}}\|_{\mathrm{F}})^{-2}$ [13]–[15] by excluding the effect of the noise. The received signal at the destination is given by $\boldsymbol{Y}_{\mathrm{RD}} = \boldsymbol{H}_{\mathrm{RD}} G_{\mathsf{SA}} \tilde{\boldsymbol{X}} + \boldsymbol{W}_{\mathrm{RD}}$, where $\tilde{\boldsymbol{X}}$ is the re-encoded OSTBC at the relay after using the squaring approach[3], whose element is the linear combination of y_k and y_k^* for $k = 1, 2, \ldots, N$. The end-to-end SNR is given by [13]–[15]

$$\gamma_{\mathsf{SA}} = \frac{\bar{\gamma}}{\mathcal{R}_c n_{\mathsf{S}}} \times \frac{\|\boldsymbol{H}_{\mathrm{SR}}\|_{\mathrm{F}}^2 \|\boldsymbol{H}_{\mathrm{RD}}\|_{\mathrm{F}}^2}{\|\boldsymbol{H}_{\mathrm{SR}}\|_{\mathrm{F}}^2 + \|\boldsymbol{H}_{\mathrm{RD}}\|_{\mathrm{F}}^2}. \tag{3}$$

If $n_{\mathsf{R}} = 1$, it can be shown that the SNR expression given in (3) is equivalent to (2). This demonstrates that the two approaches exhibit the same performance when the system has a single-antenna relay. In the existing literature, to the best of the authors' knowledge, there is no comparison between the two approaches, even for the widely treated case of Rayleigh fading.

C. Keyhole Models and Statistics of $\|\boldsymbol{H}_{\mathrm{RD}}\|_{\mathrm{F}}^2$ and $\|\boldsymbol{H}_{\mathrm{SR}}\|_{\mathrm{F}}^2$

In this subsection, we first introduce the keyhole model adopted in this paper and some statistical properties of the two random variables (RVs) $\|\boldsymbol{H}_{\mathrm{RD}}\|_{\mathrm{F}}^2$ and $\|\boldsymbol{H}_{\mathrm{SR}}\|_{\mathrm{F}}^2$ which will be helpful for asymptotic SEP derivation.

1) Single Keyhole Effect: For this scenario, we assume that the relay terminal together with the source BS is part of a fixed infrastructure network, i.e., the relay has been installed at a strategic location by the network operator [7]–[9]. Hence, the $\mathsf{S} \to \mathsf{R}$ link enjoys a rich-scattering environment, yielding the channel gain matrix $\boldsymbol{H}_{\mathrm{SR}}$ to be of full rank. On the other hand, in downlink systems, D is considered as a mobile station (MS) and applicable to be in a poor scattering environment. In order to model this practical scenario of interest, we assume that the $\mathsf{R} \to \mathsf{D}$ link is a keyhole channel, i.e., $\boldsymbol{H}_{\mathrm{RD}}$ is of unit rank. With the keyhole assumption, the channel matrix $\boldsymbol{H}_{\mathrm{RD}}$ can be mathematically described as [21] $\boldsymbol{H}_{\mathrm{RD}} = \Omega_2 \boldsymbol{x}_{\mathrm{RD}} \boldsymbol{y}_{\mathrm{RD}}^{\dagger}$. Here, $\boldsymbol{x}_{\mathrm{RD}} \in \mathbb{C}^{n_{\mathsf{D}}}$ and $\boldsymbol{y}_{\mathrm{RD}} \in \mathbb{C}^{n_{\mathsf{R}}}$ describe the scattering environment at the destination and relay, respectively [21].

2) Double Keyhole Effect: In some unplanned situations, the deployment of the relay may be more or less ad hoc, e.g., the relay may be placed based on a rough knowledge of the coverage issues and traffic density (hotspots) in the network. In such cases, both hops can be subject to poor scattering and thus we assume that both the $\boldsymbol{H}_{\mathrm{SR}}$ and $\boldsymbol{H}_{\mathrm{RD}}$ links of the network are under the influence of the keyhole effect. In this case, since the first-hop channel is now also under the keyhole effect, the corresponding channel matrix therefore can be expressed as $\boldsymbol{H}_{\mathrm{SR}} = \sqrt{\Omega_1} \boldsymbol{x}_{\mathrm{SR}} \boldsymbol{y}_{\mathrm{SR}}^{\dagger}$, where $\boldsymbol{x}_{\mathrm{SR}} \in \mathbb{C}^{n_{\mathsf{R}}}$, $\boldsymbol{y}_{\mathrm{SR}} \in \mathbb{C}^{n_{\mathsf{S}}}$ are independent random vectors constituting the scattering environment at the relay and source, respectively [21]. It is important to note that for the case of the linear approach, the current form of γ_{LA} given in (1) is too complicated to be used for performance evaluation due to the unit-rank property of $\boldsymbol{H}_{\mathrm{SR}}$. Fortunately, we can utilize the unit-rank property to simplify the complex form given in (1), which facilitates our analysis. The derivation steps are shown in the sequel.

Since $\boldsymbol{H}_{\mathrm{SR}} = \sqrt{\Omega_1} \boldsymbol{x}_{\mathrm{SR}} \boldsymbol{y}_{\mathrm{SR}}^{\dagger}$, the SNR given in (1) can be rewritten as

$$\gamma_{\mathsf{LA}} = \frac{\bar{\gamma}}{\mathcal{R}_c n_{\mathsf{S}}} G_{\mathsf{LA}}^2 \Omega_1 \|\boldsymbol{y}_{\mathrm{SR}}\|_{\mathrm{F}}^2 \operatorname{tr}\left(\boldsymbol{A} \boldsymbol{x}_{\mathrm{SR}} \boldsymbol{x}_{\mathrm{SR}}^{\dagger}\right), \tag{4}$$

[3]In this paper, we apply the general OSTBC construction with the minimum delay and maximum achievable rate proposed in [20]. The code rates at S and R are given by $\frac{\lceil \log_2(n_{\mathsf{S}}) \rceil + 1}{2^{\lceil \log_2(n_{\mathsf{S}}) \rceil}}$ and $\frac{\lceil \log_2(n_{\mathsf{R}}) \rceil + 1}{2^{\lceil \log_2(n_{\mathsf{R}}) \rceil}}$, respectively, where $\lceil \cdot \rceil$ denotes the ceiling function.

where $\boldsymbol{A} = \boldsymbol{H}_{\mathrm{RD}}^{\dagger}\left(\boldsymbol{I}_{n_{\mathsf{D}}} + G_{\mathsf{LA}}^2 \boldsymbol{H}_{\mathrm{RD}}\boldsymbol{H}_{\mathrm{RD}}^{\dagger}\right)^{-1}\boldsymbol{H}_{\mathrm{RD}}$. Owing to the fact that $\boldsymbol{A}$ is a positive definite matrix, we can apply the eigen-decomposition yielding $\boldsymbol{A} = \boldsymbol{U}\boldsymbol{\Lambda}\boldsymbol{U}^{\dagger}$ where $\boldsymbol{U}$ is a unitary matrix and $\boldsymbol{\Lambda}$ is the diagonal matrix containing the eigenvalues of $\boldsymbol{A}$. Since $\boldsymbol{H}_{\mathrm{RD}} = \sqrt{\Omega_2}\boldsymbol{x}_{\mathrm{RD}}\boldsymbol{y}_{\mathrm{RD}}^{\dagger}$ is a unit-rank matrix, $\boldsymbol{A}$ has only one non-zero eigenvalue denoted as $\frac{1}{G_{\mathsf{LA}}^2 + 1/\|\boldsymbol{H}_{\mathrm{RD}}\|_{\mathrm{F}}^2}$, leading (4) to become

$$\gamma_{\mathsf{LA}} = \frac{\bar{\gamma}\Omega_1}{\mathcal{R}_c n_{\mathsf{S}}} \times \frac{|z|^2 \|\boldsymbol{y}_{\mathrm{SR}}\|_{\mathrm{F}}^2 \|\boldsymbol{H}_{\mathrm{RD}}\|_{\mathrm{F}}^2}{\|\boldsymbol{H}_{\mathrm{RD}}\|_{\mathrm{F}}^2 + 1/G_{\mathsf{LA}}^2}, \tag{5}$$

where z is the first element of vector $\tilde{\boldsymbol{x}}_{\mathrm{SR}}$, with $\tilde{\boldsymbol{x}}_{\mathrm{SR}} = \boldsymbol{U}^{\dagger}\boldsymbol{x}_{\mathrm{SR}}$. Since $\boldsymbol{U}$ is a unitary matrix and $\boldsymbol{x}_{\mathrm{SR}} \sim \tilde{\mathcal{N}}_{n_{\mathsf{R}}}(\boldsymbol{0}, \boldsymbol{I}_{n_{\mathsf{R}}})$, we can easily see that $\tilde{\boldsymbol{x}}_{\mathrm{SR}} \sim \tilde{\mathcal{N}}_{n_{\mathsf{R}}}(\boldsymbol{0}, \boldsymbol{I}_{n_{\mathsf{R}}})$ leads to $z \sim \mathcal{CN}(0,1)$. As compared to (1), the new expression of γ_{LA} is more tractable.

3) Statistics of $\|\boldsymbol{H}_{\mathrm{RD}}\|_{\mathrm{F}}^2$ and $\|\boldsymbol{H}_{\mathrm{SR}}\|_{\mathrm{F}}^2$: The statistics of $\|\boldsymbol{H}_{\mathrm{RD}}\|_{\mathrm{F}}^2$ and $\|\boldsymbol{H}_{\mathrm{SR}}\|_{\mathrm{F}}^2$ applicable under keyhole conditions will be utilized in our subsequent performance analysis. Due to symmetry between $\|\boldsymbol{H}_{\mathrm{RD}}\|_{\mathrm{F}}^2$ and $\|\boldsymbol{H}_{\mathrm{SR}}\|_{\mathrm{F}}^2$, let us denote $\mathsf{AB} \in \{\mathsf{SR}, \mathsf{RD}\}$ and $\ell \in \{1,2\}$ for the sake of brevity. Since $\boldsymbol{H}_{\mathrm{AB}} = \sqrt{\Omega_\ell}\boldsymbol{x}_{\mathrm{AB}}\boldsymbol{y}_{\mathrm{AB}}^{\dagger}$, we then can express $\|\boldsymbol{H}_{\mathrm{AB}}\|_{\mathrm{F}}^2 = \Omega_\ell \|\boldsymbol{x}_{\mathrm{AB}}\|_{\mathrm{F}}^2 \|\boldsymbol{y}_{\mathrm{AB}}\|_{\mathrm{F}}^2$. As $\boldsymbol{x}_{\mathrm{AB}}$ and $\boldsymbol{y}_{\mathrm{AB}}$ are statistically independent, the PDF of $\|\boldsymbol{H}_{\mathrm{AB}}\|_{\mathrm{F}}^2$ when subject to the keyhole effect is given by [4]

$$f_{\|\boldsymbol{H}_{\mathrm{AB}}\|_{\mathrm{F}}^2}(z) = \frac{2z^{(n_{\mathsf{A}}+n_{\mathsf{B}})/2-1}}{\Gamma(n_{\mathsf{A}})\Gamma(n_{\mathsf{B}})\Omega_\ell^{(n_{\mathsf{A}}+n_{\mathsf{B}})/2}}\mathcal{K}_{n_{\mathsf{B}}-n_{\mathsf{A}}}\left(2\sqrt{\frac{z}{\Omega_\ell}}\right). \tag{6}$$

Since $\|\boldsymbol{H}_{\mathrm{AB}}\|_{\mathrm{F}}^2$ is the product of two RVs, the CDF of $\|\boldsymbol{H}_{\mathrm{AB}}\|_{\mathrm{F}}^2$ can be written as $F_{\|\boldsymbol{H}_{\mathrm{AB}}\|_{\mathrm{F}}^2}(z) = \int_0^{\infty} f_{\|\boldsymbol{x}_{\mathrm{AB}}\|_{\mathrm{F}}^2}(w) F_{\|\boldsymbol{y}_{\mathrm{AB}}\|_{\mathrm{F}}^2}\left(\frac{z}{\Omega_\ell w}\right) dw$. Note that the CDF of $\|\boldsymbol{y}_{\mathrm{AB}}\|_{\mathrm{F}}^2$ can be given in the form of elementary functions by applying [18, Eq. (8.352.4)]. Then, utilizing the result of [18, Eq. (3.471.9)], we get the CDF of $\|\boldsymbol{H}_{\mathrm{AB}}\|_{\mathrm{F}}^2$ as

$$F_{\|\boldsymbol{H}_{\mathrm{AB}}\|_{\mathrm{F}}^2}(z) = 1 - \sum_{k=1}^{n_{\mathsf{A}}-1} \frac{2}{\Gamma(n_{\mathsf{B}})k!}\left(\frac{z}{\Omega_\ell}\right)^{(n_{\mathsf{B}}+k)/2} \times \mathcal{K}_{n_{\mathsf{B}}-k}\left(2\sqrt{\frac{z}{\Omega_\ell}}\right). \tag{7}$$

III. High-SNR SEP Analysis

It is noted that for the considered SKE and DKE cases, an exact closed-form SEP analysis is not possible. Moreover, using our subsequent analysis, the exact SEP can be evaluated using numerical integration. In order to obtain key insights and how different parameters affect the system performance, we therefore investigate the high SNR SEP behavior that yields the array and diversity gains of MIMO AF systems with the keyhole effect. Specifically, in the case of SKE with LA, we use exact SEP expression [11], which is given in the form of a finite integral whose integrand is the MGF function of the SNR, to obtain the asymptotic SEP. In the cases of: (1) SKE with SA and (2) DKE with SA, we utilize an asymptotic analysis as in [22] to obtain a polynomial approximation to the exact SEP in the high SNR regime. In the case of DKE with LA, we obtain the desired diversity order result using an upper and a lower bound to the exact end-to-end SNR.

A. Single Keyhole Effect with Linear Approach

For the dual-hop MIMO AF relaying with linear approach, from (1), the moment generating function (MGF) can be obtained from the definition $\mathcal{M}_{\mathsf{LA}}(s) = \mathbb{E}_{\gamma_{\mathsf{LA}}}\{e^{-s\gamma_{\mathsf{LA}}}\}$ as [10], [11]

$$\mathcal{M}_{\mathsf{LA}}(s) = \mathbb{E}_{\boldsymbol{H}_{\mathrm{RD}}}\left\{\left(\frac{\det\left(\boldsymbol{I}_{n_{\mathsf{D}}} + G_{\mathsf{LA}}^2\boldsymbol{H}_{\mathrm{RD}}\boldsymbol{H}_{\mathrm{RD}}^{\dagger}\right)}{\det\left(\boldsymbol{I}_{n_{\mathsf{D}}} + G_{\mathsf{LA}}^2\left(1 + \frac{s\bar{\gamma}\Omega_1}{\mathcal{R}_c n_{\mathsf{S}}}\right)\boldsymbol{H}_{\mathrm{RD}}\boldsymbol{H}_{\mathrm{RD}}^{\dagger}\right)}\right)^{n_{\mathsf{S}}}\right\}. \tag{8}$$

Let us denote x as a non-zero eigenvalue of $\boldsymbol{H}_{\mathrm{RD}}\boldsymbol{H}_{\mathrm{RD}}^{\dagger}$. Since $\boldsymbol{H}_{\mathrm{RD}}$ is of unit rank, it is easy to see that there exists only one non-zero eigenvalue of $x = \|\boldsymbol{H}_{\mathrm{RD}}\|_{\mathrm{F}}^2$. Using this property and from (6), we can rewrite (8) as

$$\mathcal{M}_{\gamma_{\mathsf{LA}}}(s) = \int_0^{\infty} \frac{2(\Omega_2\bar{\gamma})^{-(n_{\mathsf{R}}+n_{\mathsf{D}})/2}}{\Gamma(n_{\mathsf{R}})\Gamma(n_{\mathsf{D}})}\left[1 + \frac{G_{\mathsf{LA}}^2\Omega_1 st}{\mathcal{R}_c n_{\mathsf{S}}\left(1 + G_{\mathsf{LA}}^2\bar{\gamma}^{-1}t\right)}\right]^{-n_{\mathsf{S}}} \times t^{(n_{\mathsf{R}}+n_{\mathsf{D}})/2-1}\mathcal{K}_{n_{\mathsf{D}}-n_{\mathsf{R}}}\left(2\sqrt{\frac{t}{\bar{\gamma}\Omega_2}}\right)dt. \tag{9}$$

To the best of the authors' knowledge, (9) has no closed-form solution. As a result, we present the asymptotic SEP for single keyhole effect with linear approach in the following Theorem.

Theorem 1: In the high SNR regime, the SEP expression for MIMO AF relaying with linear approach and single keyhole effect can be given by

$$P_{\mathrm{e}}^{(\mathsf{SRD})} \overset{(\text{large } \bar{\gamma})}{\approx} c_1\left(\frac{\Omega_1\Omega_2 G_{\mathsf{LA}}^2\bar{\gamma}}{\mathcal{R}_c n_{\mathsf{S}}}\right)^{-\min(n_{\mathsf{R}},n_{\mathsf{D}})} \times \frac{\Gamma(n_{\mathsf{S}} - \min(n_{\mathsf{R}},n_{\mathsf{D}}))\Gamma(\min(n_{\mathsf{R}},n_{\mathsf{D}}))}{\Gamma(n_{\mathsf{S}})\Gamma(n_{\mathsf{R}})\Gamma(n_{\mathsf{D}})} \tag{10}$$

with the condition that $n_{\mathsf{S}} > \min(n_{\mathsf{R}}, n_{\mathsf{D}})$ and c_1 is a constant depending on the modulation scheme. For example, for M-PSK modulation, c_1 is defined as

$$c_1 = \begin{cases} \frac{1}{\pi}\int_0^{\pi-\frac{\pi}{M}}\left(\frac{\mathrm{g}}{\sin^2\theta}\right)^{-n_{\mathsf{R}}}\left[\ln\left(\frac{\Omega_1\Omega_2 G_{\mathsf{LA}}^2\bar{\gamma}\mathrm{g}}{\mathcal{R}_c n_{\mathsf{S}}\sin^2\theta}\right) - \psi(n_{\mathsf{R}}) + \psi(n_{\mathsf{S}} - n_{\mathsf{R}})\right]d\theta, & \text{for } n_{\mathsf{R}} = n_{\mathsf{D}}, \\ \frac{\Gamma(|n_{\mathsf{D}} - n_{\mathsf{R}}|)}{\pi} \times \int_0^{\pi-\frac{\pi}{M}}\left(\frac{\mathrm{g}}{\sin^2\theta}\right)^{-\min(n_{\mathsf{R}},n_{\mathsf{D}})}d\theta, & \text{for } n_{\mathsf{R}} \neq n_{\mathsf{D}}. \end{cases} \tag{11}$$

Proof: See Appendix A. ■

Since we consider downlink communication, it is reasonable to assume that $n_{\mathsf{S}} > n_{\mathsf{D}}$. As can be observed from (10), the SEP is inversely proportional to $\bar{\gamma}^{\min(n_{\mathsf{R}},n_{\mathsf{D}})}$[4]. Hence, the full achievable diversity gain provided by the fixed relay link using linear approach is $\min(n_{\mathsf{R}}, n_{\mathsf{D}})$. In addition, as can be observed from (10), the array gain can be clearly obtained.

B. Double Keyhole Effect with Linear Approach

In the case of the double keyhole channel, as can be seen from (5), the exact PDF derivation of γ_{LA} requires the statistics of multiple products and division of RVs. In the considered problem, these expressions are not trivial to obtain and do

[4]Although the asymptotic SEP is given in the form of the product of polynomial and logarithm functions with respect to the average SNR $\bar{\gamma}$ [23], [24], the diversity order is solely determined by the polynomial term since $\frac{\log\log\bar{\gamma}}{\log\bar{\gamma}}$ can be neglected as $\bar{\gamma} \to \infty$.

not lend mathematical tractability for further manipulation. Therefore, we will utilize the upper and lower bounds of γ_{LA} for the analysis instead. Using (5), the instantaneous end-to-end SNR when both hops undergo keyhole can be rewritten as $\gamma_{\mathsf{LA}} = \left(\frac{1}{\gamma_1} + \frac{c_2}{\gamma_1\gamma_2}\right)^{-1}$, where $c_2 = \bar{\gamma}/G_{\mathsf{LA}}^2$, $\gamma_1 = \frac{\Omega_1\bar{\gamma}}{\mathcal{R}_c n_{\mathsf{S}}}|z|^2 \left\|\boldsymbol{y}_{\mathrm{SR}}\right\|_{\mathrm{F}}^2$, and $\gamma_2 = \bar{\gamma}\left\|\boldsymbol{H}_{\mathrm{RD}}\right\|_{\mathrm{F}}^2$. Hence, it is convenient for us to introduce the lower and upper bounds of γ_{LA} as

$$\gamma_{\mathsf{LA}}^{(\mathsf{lo})} \triangleq \frac{1}{2}\min(\gamma_1, \frac{\gamma_1\gamma_2}{c_2}) \leq \gamma_{\mathsf{LA}} \leq \min(\gamma_1, \frac{\gamma_1\gamma_2}{c_2}) \triangleq \gamma_{\mathsf{LA}}^{(\mathsf{up})}. \tag{12}$$

Theorem 2: In the high SNR regime, the SEP expression for MIMO AF relaying with linear approach and double keyhole effect can be lower and upper bounded as

$$\frac{c_3}{\bar{\gamma}} \leq P_{\mathrm{e}}^{(\mathsf{SRD})} \leq \frac{2c_3}{\bar{\gamma}}, \tag{13}$$

where

$$c_3 = \left[\frac{\epsilon}{\Omega_2 G_{\mathsf{LA}}^2 (n_{\mathsf{R}}-1)(n_{\mathsf{D}}-1)} + \bar{\epsilon}\right] \frac{\mathcal{R}_c n_{\mathsf{S}}}{\Omega_1 (n_{\mathsf{S}}-1)\pi \mathsf{g}} \times \left[\frac{(M-1)\pi}{2M} + \frac{\sin(2\pi/M)}{4M}\right]. \tag{14}$$

Proof: See Appendix B. ■

Based on (13), we can observe that the slope of the SEP curve in the high SNR regime is one. In other words, when both hops experience the keyhole effect, a relay using the linear approach exhibits an unit diversity order regardless of the number of antennas.

C. Single Keyhole Effect with Squaring Approach

With the squaring approach, the instantaneous SNR incurred by the dual-hop channel can be given in the form of the harmonic mean of two independent RVs as in (3) and rewritten as follows:

$$\gamma_{\mathsf{SA}} = \frac{1}{\mathcal{R}_c n_{\mathsf{S}}} \frac{\gamma_2\gamma_3}{\gamma_2+\gamma_3}, \tag{15}$$

where $\gamma_3 = \bar{\gamma}\left\|\boldsymbol{H}_{\mathrm{SR}}\right\|_{\mathrm{F}}^2$. In this case, since the first hop, i.e., $\mathsf{S} \to \mathsf{R}$, is keyhole-free, the squared Frobenius norm of $\boldsymbol{H}_{\mathrm{SR}}$, $\left\|\boldsymbol{H}_{\mathrm{SR}}\right\|_{\mathrm{F}}^2$, is the sum of $n_{\mathsf{S}}n_{\mathsf{R}}$ independent and identically distributed exponential RVs. Then, the asymptotic PDF of γ_3 can be given as [22]

$$f_{\gamma_3}(\gamma_3) \overset{(\text{large } \bar{\gamma})}{\approx} \frac{\gamma_3^{n_{\mathsf{S}}n_{\mathsf{R}}-1}}{\Gamma(n_{\mathsf{S}}n_{\mathsf{R}})(\bar{\gamma})^{n_{\mathsf{S}}n_{\mathsf{R}}-1}}. \tag{16}$$

Depending on the relationship between n_{R} and n_{D}, the asymptotic SEP expression for MIMO AF relaying with squaring approach and single keyhole effect can be presented in the following Theorem.

Theorem 3: When $n_{\mathsf{R}} \neq n_{\mathsf{D}}$, in the high SNR regime, the asymptotic SEP is written as

$$P_{\mathrm{e}}^{(\mathsf{SRD})} \overset{(\text{large } \bar{\gamma})}{\approx} \frac{\prod_{i=1}^{\min(n_{\mathsf{R}},n_{\mathsf{D}})}(2i-1)}{\min(n_{\mathsf{R}},n_{\mathsf{D}})} \frac{\Gamma(|n_{\mathsf{D}}-n_{\mathsf{R}}|)}{\Gamma(n_{\mathsf{R}})\Gamma(n_{\mathsf{D}})} \times \left(\frac{\mathcal{R}_c n_{\mathsf{S}}}{2\mathsf{g}\Omega_2\bar{\gamma}}\right)^{\min(n_{\mathsf{R}},n_{\mathsf{D}})}. \tag{17}$$

When $n_{\mathsf{R}} = n_{\mathsf{D}}$, in the high SNR regime, the SEP can be upper and lower bounded as

$$\frac{c_4(1)}{\bar{\gamma}^{n_{\mathsf{R}}}} \leq P_{\mathrm{e}}^{(\mathsf{SRD})} \leq \frac{c_4(2)}{\bar{\gamma}^{n_{\mathsf{R}}}}, \tag{18}$$

where $c_4(\star)$ is a constant expressed as

$$c_4(\star) = \frac{1}{\pi\Gamma(n_{\mathsf{R}})}\left(\frac{\mathcal{R}_c n_{\mathsf{S}}}{\Omega_2\mathsf{g}}\right)^{n_{\mathsf{R}}} \int_0^{\pi-\pi/M} \left(\star\sin^2\theta\right)^{n_{\mathsf{R}}} \times \left[\ln\left(\frac{\Omega_2\bar{\gamma}\mathsf{g}}{\star\mathcal{R}_c n_{\mathsf{S}}\sin^2\theta}\right) - \psi(n_{\mathsf{R}})\right] d\theta. \tag{19}$$

Proof: See Appendix C. ■

By combining (17) and (18), we see that when the fixed relay terminal uses the squaring approach, the full achievable diversity order is $\min(n_{\mathsf{R}}, n_{\mathsf{D}})$.

D. Double Keyhole Effect with Squaring Approach

In this case where both hops are subject to the keyhole effect, the PDF and CDF of γ_3 can be obtained from (6) and (7), respectively, by applying a Jacobian transformation. Since we consider a downlink communication scenario, i.e., $n_{\mathsf{S}} > n_{\mathsf{R}}$, from (25) the asymptotic $f_{\gamma_3}(\gamma)$ can be derived as

$$f_{\gamma_3}(\gamma) \overset{(\text{large } \bar{\gamma})}{\approx} \frac{\Gamma(n_{\mathsf{S}}-n_{\mathsf{R}})}{\Gamma(n_{\mathsf{S}})\Gamma(n_{\mathsf{R}})} \frac{\gamma^{n_{\mathsf{R}}-1}}{(\Omega_1\bar{\gamma})^{n_{\mathsf{R}}}}. \tag{20}$$

Again, similarly as in Sections III-A, III-B, and III-C, by distinguishing separate cases due to the approximation of the modified Bessel function of the second kind, the asymptotic SEP expression for MIMO AF relaying with squaring approach and double keyhole effect can be presented in the following Theorem.

Theorem 4: In the high SNR regime, the asymptotic SEP expression can be derived for the cases $n_{\mathsf{R}} > n_{\mathsf{D}}$ and $n_{\mathsf{R}} < n_{\mathsf{D}}$, respectively, as follows:

$$P_{\mathrm{e}}^{(\mathsf{SRD})} \overset{(\text{large } \bar{\gamma})}{\approx} \frac{\prod_{i=1}^{n_{\mathsf{D}}}(2i-1)\Gamma(n_{\mathsf{R}}-n_{\mathsf{D}})}{\Gamma(n_{\mathsf{R}})\Gamma(n_{\mathsf{D}}+1)} \left(\frac{\mathcal{R}_c n_{\mathsf{S}}}{2\mathsf{g}\Omega_2\bar{\gamma}}\right)^{n_{\mathsf{D}}}. \tag{21}$$

$$P_{\mathrm{e}}^{(\mathsf{SRD})} \overset{(\text{large } \bar{\gamma})}{\approx} \frac{\prod_{i=1}^{n_{\mathsf{R}}}(2i-1)}{\Gamma(n_{\mathsf{R}}+1)} \left[\frac{\Gamma(n_{\mathsf{D}}-n_{\mathsf{R}})}{\Gamma(n_{\mathsf{D}})\Omega_2^{n_{\mathsf{R}}}} + \frac{\Gamma(n_{\mathsf{S}}-n_{\mathsf{R}})}{\Gamma(n_{\mathsf{S}})\Omega_1^{n_{\mathsf{R}}}}\right] \times \left(\frac{\mathcal{R}_c n_{\mathsf{S}}}{2\mathsf{g}\bar{\gamma}}\right)^{n_{\mathsf{R}}}. \tag{22}$$

When $n_{\mathsf{R}} = n_{\mathsf{D}}$, in the high SNR regime, the SEP expression can be lower and upper bounded as

$$\frac{c_5(1)}{\bar{\gamma}^{n_{\mathsf{R}}}} \leq P_{\mathrm{e}}^{(\mathsf{SRD})} \leq \frac{c_5(2)}{\bar{\gamma}^{n_{\mathsf{R}}}}, \tag{23}$$

where $c_5(\star)$ is a constant given by

$$c_5(\star) = \frac{(\mathcal{R}_c n_{\mathsf{S}})^{n_{\mathsf{R}}}}{\pi\Gamma(n_{\mathsf{R}})} \int_0^{\pi-\pi/M} \left(\frac{\star\sin^2\theta}{\mathsf{g}}\right)^{n_{\mathsf{R}}} \times \left[\frac{\ln\left(\frac{\Omega_1\bar{\gamma}\mathsf{g}}{\star\mathcal{R}_c n_{\mathsf{S}}\sin^2\theta}\right) - \psi(n_{\mathsf{R}})}{\Omega_2^{n_{\mathsf{R}}}} + \frac{\Gamma(n_{\mathsf{S}}-n_{\mathsf{R}})}{\Omega_1^{n_{\mathsf{R}}}}\right] d\theta. \tag{24}$$

Proof: See Appendix D. ■

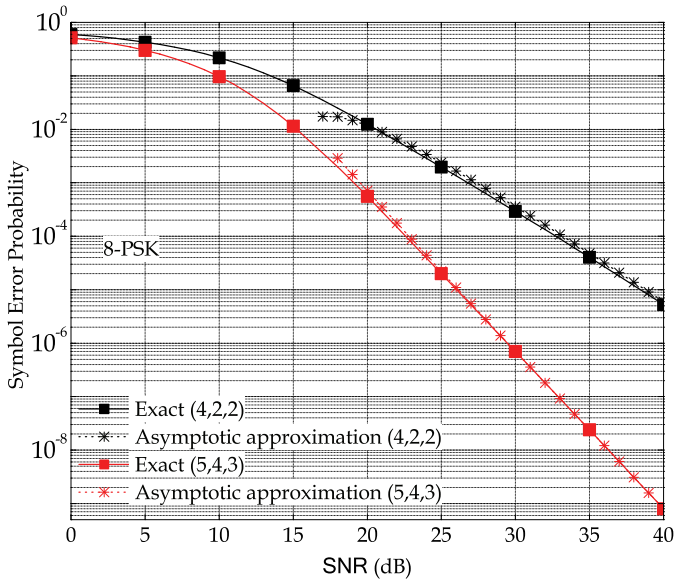

Fig. 2. SEP of $(4, 2, 2)$ and $(5, 4, 3)$-MIMO AF relay systems for 8-PSK modulation versus SNR when only the second hop experiences the keyhole effect and the relay uses the linear approach.

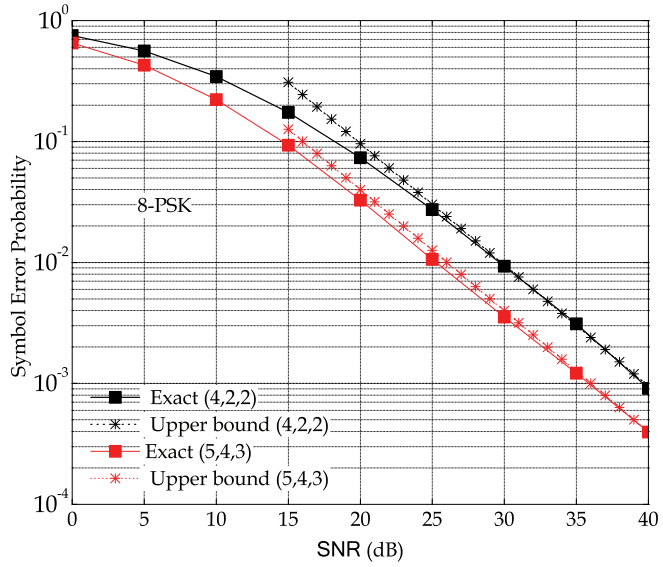

Fig. 3. SEP of $(4, 2, 2)$ and $(5, 4, 3)$-MIMO AF relay systems for 8-PSK modulation versus SNR when both hops experience keyhole effect and the relay uses the linear approach.

By combining (21), (22), and (23), we can observe that the diversity order is $\min(n_{\mathsf{R}}, n_{\mathsf{D}})$. Therefore, compared with the unit diversity order achieved with the linear approach (cf. Section III-B), a larger diversity order can be achieved with the squaring approach.

IV. Numerical Results and Discussion

In this section, we investigate the keyhole effect on the SEP performance of OSTBC MIMO AF relaying with the help of the analytical derivation developed in Section III. To illustrate the correctness of the asymptotic result, we also provide exact numerical results, which are obtained from numerical integration. For example, in the case of fixed relay with the linear approach, from (9), we can evaluate the exact SEP using numerical integration techniques. However, these SEP expressions are in the form of double or triple integrals and do not reveal any insight into the system performance. Moreover, simulation results also confirm our analytical results but are not shown here to avoid clutter in the figures. In all examples, results are shown for 8-PSK modulation and unit variances $(\Omega_1 = \Omega_2 = 1)$. We consider different numbers of antennas at S, R, D denoted as $(n_{\mathsf{S}}, n_{\mathsf{R}}, n_{\mathsf{D}})$, where $n_{\mathsf{S}} > \min(n_{\mathsf{R}}, n_{\mathsf{D}})$. In addition, the OSTBCs are generated from [20], e.g., the code-rates for the case of two and three transmit antennas are one and 3/4, respectively.

For the linear approach, the SEP when only the second hop experiences the keyhole effect is shown in Fig. 2, where we compare asymptotic SEP with exact numerical results for two different antenna configurations, e.g., $(4, 2, 2)$ and $(5, 4, 3)$. As expected, the asymptotic curves exactly converge to the exact curves in the high SNR regime. We can see that the slopes of SEP curves are regulated by the minimum number of antennas at the relay and destination. Fig. 3 displays the SEP performance with DKE and the squaring approach. We have plotted the upper asymptotic bounds for the two different MIMO AF relay systems as in the above example. Clearly, as observed from the plots, the upper bound becomes very tight in the high SNR regime and can be considered as the asymptotic SEP. For further comparison, the two systems exhibit the same diversity gain as expected. We see that as the number of antennas increases, i.e., from $(4, 2, 2)$ to $(5, 4, 3)$, the slopes of SEP curves remain unchanged and equal to one, which agrees with our analytical conclusion in Section III-C.

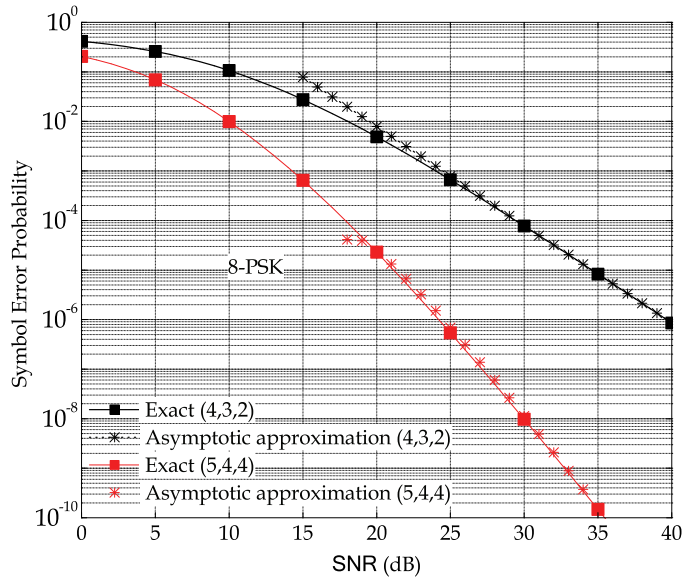

Fig. 4. SEP of $(4, 3, 2)$ and $(5, 4, 4)$-MIMO AF relay systems for 8-PSK modulation versus SNR when only the second hop experiences the keyhole effect and the relay uses the squaring approach.

For the squaring approach, Fig. 4 shows the SEP performance of the two different MIMO AF relay systems, i.e., $(4, 3, 2)$ and $(5, 4, 4)$, when only the second hop experiences the keyhole effect. The SEP performance improves as the $\min(n_{\mathsf{R}}, n_{\mathsf{D}})$ increases. Again, we observe an excellent agreement between the asymptotic and exact curves in the high SNR regime. In Fig. 5, we plot the average SEP when both hops

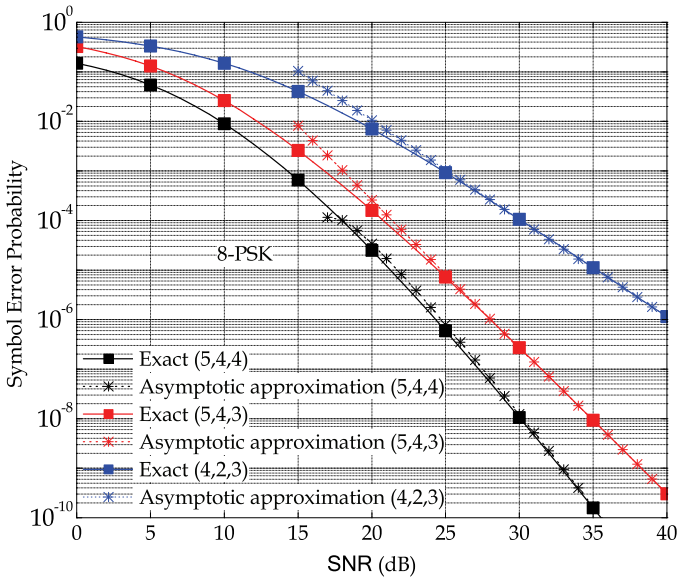

Fig. 5. SEP of $(4,2,3)$, $(5,4,3)$, and $(5,4,4)$-MIMO AF relay systems for 8-PSK modulation versus SNR when both hops experience the keyhole effect and the relay uses the squaring approach.

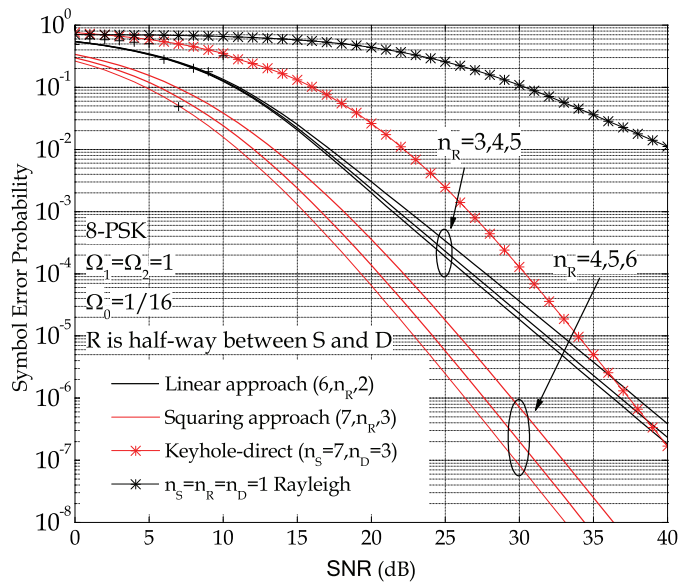

Fig. 6. SEP of $(6, n_{\mathsf{R}}, 2)$ and $(7, n_{\mathsf{R}}, 3)$-MIMO AF relay systems for 8-PSK modulation versus SNR when only the second hop experiences the keyhole effect. For comparison, SEPs for direct link with keyhole and single antenna relaying link are also shown.

are subject to keyhole fading. Three specific system configurations, i.e., $(5,4,4)$, $(5,4,3)$, and $(4,2,3)$, corresponding to the three conditions in the Section III-D (i.e., $n_{\mathsf{R}} = n_{\mathsf{D}}$, $n_{\mathsf{R}} > n_{\mathsf{D}}$, and $n_{\mathsf{R}} < n_{\mathsf{D}}$), are used. In the three cases, our asymptotic results are seen to converge to the respective exact curves for relatively high SNR levels (SNR $>$ 20 dB). As expected, the best performance among the three examples is achieved for $(5,4,4)$.

To further demonstrate the cooperative diversity derived in the previous section, we plot the SEP for $(6, n_{\mathsf{R}}, 2)$ with the linear approach and varying n_{R} from three to five and for $(7, n_{\mathsf{R}}, 3)$ with the squaring approach and varying n_{R} from four to six. For comparison, we also plot the SEP for single-hop non-cooperative communications with keyhole and the SEP for single antenna relay. Here, we assume that R is located half-way between S and D, which results in the channel mean power for the direct link as $\Omega_0 = 1/16$. As can be observed from Fig. 6, increasing the number of antennas at relays while keeping n_{D} unchanged results in no diversity enhancement. This observation is in line with our analytical result derived in the previous section as the full achievable diversity gain is $\min(n_{\mathsf{R}}, n_{\mathsf{D}})$. In fact, under such a severe condition it is unnecessary to deploy a large number of antennas at the relay, but only requiring $n_{\mathsf{R}} = n_{\mathsf{D}}$. More importantly, we can see that direct communication, i.e., $(n_{\mathsf{S}}, n_{\mathsf{D}}) = (7,3)$, exhibits the same diversity gain as MIMO AF relaying with the squaring approach, i.e., $(7, n_{\mathsf{R}}, 3)$. However, relaying link with the squaring approach significantly outperforms the direct link in terms of array gain. Also, when SNR$\leq$ 35 dB the SEP of direct communication is inferior to that of MIMO AF relay with the linear approach, which clearly highlights the advantage of using relays in keyhole fading.

V. Conclusion

We have investigated the effect of keyhole on the performance of downlink AF relay systems with OSTBC transmission. In particular, we have investigated the effect of keyhole on the SEP performance when the AF relay operates in either linear or squaring approaches. Our tractable asymptotic SEP expressions reveal both diversity and array gains and provide important insights for radio system designers. For the case when only the second hop suffers from the keyhole effect, we have suggested to apply the linear approach at the relay for obtaining the full achievable diversity gain of $\min(n_{\mathsf{R}}, n_{\mathsf{D}})$ while keeping low complexity for the relay. In contrast, for a more severe scenario where both hops are keyhole channels, the squaring approach should be used to keep the diversity order as $\min(n_{\mathsf{R}}, n_{\mathsf{D}})$ since the linear approach does not offer any diversity gain.

Appendix A: Proof of Theorem 1

To study the high SNR performance, we make use of the fact that for small values of z, $\mathcal{K}_n(z)$ can be approximated as [25]

$$\mathcal{K}_n(z) \overset{(\text{small } z)}{\approx} \begin{cases} \ln\left(\frac{2}{z}\right) & \text{for } n = 0, \\ \frac{\Gamma(|n|)}{2}\left(\frac{2}{z}\right)^{|n|} & \text{for } n \neq 0. \end{cases} \tag{25}$$

By substituting (25) into (9), we obtain an asymptotic $\mathcal{M}_{\gamma_{\mathsf{LA}}}(s)$ in the high SNR regime. Note that depending on the value of n_{R} and n_{D}, $\mathcal{K}_{n_{\mathsf{D}}-n_{\mathsf{R}}}(\cdot)$ can be differently approximated as in (25). Therefore, we will separately investigate two cases as follows: For the case $n_{\mathsf{R}} = n_{\mathsf{D}}$, replacing $\mathcal{K}_{n_{\mathsf{D}}-n_{\mathsf{R}}}\left(2\sqrt{\frac{t}{\bar{\gamma}\Omega_2}}\right)$ by $\frac{1}{2}\ln\left(\frac{\bar{\gamma}\Omega_2}{t}\right)$ and neglecting the small term relative to $\bar{\gamma}$ in the integrand of (9) results in

$$\mathcal{M}_{\gamma_{\mathsf{LA}}}(s) \overset{(\text{large } \bar{\gamma})}{\approx} \frac{(\Omega_2\bar{\gamma})^{-n_{\mathsf{R}}}}{\Gamma(n_{\mathsf{R}})\Gamma(n_{\mathsf{D}})}\left[\int_0^\infty \frac{\ln(\Omega_2\bar{\gamma})t^{n_{\mathsf{R}}-1}}{\left(1+\frac{G_{\mathsf{LA}}^2\Omega_1 s}{\mathcal{R}_c n_{\mathsf{S}}}t\right)^{n_{\mathsf{S}}}}dt - \int_0^\infty \frac{t^{n_{\mathsf{R}}-1}\ln(t)}{\left(1+\frac{G_{\mathsf{LA}}^2\Omega_1 s}{\mathcal{R}_c n_{\mathsf{S}}}t\right)^{n_{\mathsf{S}}}}dt\right]. \tag{26}$$

The first and second integral in the above equation can be easily computed by applying the results of [18, Eq. (3.194.3)] and [26, Eq. (2.6.4.7)], respectively, with the condition that $n_{\mathsf{S}} > n_{\mathsf{R}}$. After several algebraic manipulations, the MGF of γ_{LA} can be written as

$$\mathcal{M}_{\gamma_{\mathsf{LA}}}(s) \overset{(\text{large } \bar{\gamma})}{\approx} \left(\frac{\Omega_1\Omega_2 G_{\mathsf{LA}}^2 \bar{\gamma} s}{\mathcal{R}_c n_{\mathsf{S}}}\right)^{-n_{\mathsf{R}}} \frac{\Gamma(n_{\mathsf{S}}-n_{\mathsf{R}})}{\Gamma(n_{\mathsf{S}})\Gamma(n_{\mathsf{R}})} \times \left[\ln\left(\frac{\Omega_1\Omega_2 G_{\mathsf{LA}}^2 \bar{\gamma} s}{\mathcal{R}_c n_{\mathsf{S}}}\right) - \psi(n_{\mathsf{R}}) + \psi(n_{\mathsf{S}}-n_{\mathsf{R}})\right]. \quad (27)$$

For the case $n_{\mathsf{R}} \neq n_{\mathsf{D}}$, we can find the MGF of γ_{LA} as

$$\mathcal{M}_{\gamma_{\mathsf{LA}}}(s) \overset{(\text{large } \bar{\gamma})}{\approx} \frac{(\Omega_2\bar{\gamma})^{-\min(n_{\mathsf{R}},n_{\mathsf{D}})}}{\Gamma(n_{\mathsf{R}})\Gamma(n_{\mathsf{D}})} \times \int_0^\infty t^{\min(n_{\mathsf{R}},n_{\mathsf{D}})-1}\left(1+\frac{G_{\mathsf{LA}}^2\Omega_1 s}{\mathcal{R}_c n_{\mathsf{S}}}t\right)^{-n_{\mathsf{S}}} dt. \quad (28)$$

Note that the integral (28) converges when $n_{\mathsf{S}} > \min(n_{\mathsf{R}}, n_{\mathsf{D}})$ which then yields

$$\mathcal{M}_{\gamma_{\mathsf{LA}}}(s) \overset{(\text{large } \bar{\gamma})}{\approx} \left(\frac{\Omega_1\Omega_2 G_{\mathsf{LA}}^2 \bar{\gamma} s}{\mathcal{R}_c n_{\mathsf{S}}}\right)^{-\min(n_{\mathsf{R}},n_{\mathsf{D}})} \times \frac{\Gamma(n_{\mathsf{S}}-\min(n_{\mathsf{R}},n_{\mathsf{D}}))\Gamma(\min(n_{\mathsf{R}},n_{\mathsf{D}}))\Gamma(|n_{\mathsf{D}}-n_{\mathsf{R}}|)}{\Gamma(n_{\mathsf{S}})\Gamma(n_{\mathsf{R}})\Gamma(n_{\mathsf{D}})}. \quad (29)$$

By combining the two cases and using the fact that the exact SEP of M-PSK modulation is given by [11, Eq. (21)]

$$P_{\mathrm{e}}^{(\mathsf{SRD})} = \frac{1}{\pi}\int_0^{\pi-\frac{\pi}{M}} \mathcal{M}_{\gamma_{\mathsf{LA}}}\left(\frac{\mathsf{g}}{\sin^2\theta}\right) d\theta \quad (30)$$

where $\mathsf{g} = \sin^2\left(\frac{\pi}{M}\right)$, the asymptotic SEP of a dual-hop channel, i.e., $\mathsf{S} \to \mathsf{R} \to \mathsf{D}$ link, when the fixed relay terminal operates in linear mode can be expressed as (10), which completes our proof.

Appendix B: Proof of Theorem 2

We first derive the upper bound and note that the derivation of lower bound can be followed accordingly. By definition, the CDF of $\gamma_{\mathsf{LA}}^{(\mathsf{up})}$ is given by $F_{\gamma_{\mathsf{LA}}^{(\mathsf{up})}}(\gamma) = \underbrace{\Pr\left(\gamma_1 < \gamma, \gamma_1 < \frac{\gamma_1\gamma_2}{c_2}\right) + \Pr\left(\frac{\gamma_1\gamma_2}{c_2} < \gamma, \frac{\gamma_1\gamma_2}{c_2} < \gamma_1\right)}_{\mathcal{L}}$. In addition, we have $\mathcal{L} = \Pr(\gamma_1 < \gamma, \gamma_2 < c_2) + \Pr(\gamma_1 > \gamma, \gamma_1\gamma_2 < \gamma c_2)$. As a result, the CDF of $\gamma_{\mathsf{LA}}^{(\mathsf{up})}$ can be rewritten as $F_{\gamma_{\mathsf{LA}}^{(\mathsf{up})}}(\gamma) = \underbrace{\Pr(\gamma_1 < \gamma, \gamma_2 > c_2) + \Pr(\gamma_1 < \gamma, \gamma_2 < c_2)}_{=\Pr(\gamma_1<\gamma)} + \Pr(\gamma_1 > \gamma, \gamma_1\gamma_2 < \gamma c_2)$, which then yields $F_{\gamma_{\mathsf{LA}}^{(\mathsf{up})}}(\gamma) = F_{\gamma_1}(\gamma) + \Pr\left(\gamma < \gamma_1 < \frac{\gamma c_2}{\gamma_2}\right)$. Since further manipulations of the exact $F_{\gamma_{\mathsf{LA}}^{(\mathsf{up})}}(\gamma)$ is cumbersome, we asymptotically apply the following identity

$$F_{\gamma_{\mathsf{LA}}^{(\mathsf{up})}}(\gamma) \overset{(\text{large } \bar{\gamma})}{\approx} \Pr(\gamma_2 < c_2)\Pr\left(\frac{\gamma_1\gamma_2}{c_2} < \gamma\right) + \Pr(\gamma_2 \geq c_2)\Pr(\gamma_1 < \gamma). \quad (31)$$

Since γ_1 is the product of exponent and chi-square RVs, its PDF and CDF are given by, respectively

$$f_{\gamma_1}(x) = \frac{2x^{(n_{\mathsf{S}}-1)/2}}{\Gamma(n_{\mathsf{S}})[\Omega_1\bar{\gamma}/(\mathcal{R}_c n_{\mathsf{S}})]^{(n_{\mathsf{S}}+1)/2}} \times \mathcal{K}_{n_{\mathsf{S}}-1}\left(2\sqrt{\frac{x}{\Omega_1\bar{\gamma}/(\mathcal{R}_c n_{\mathsf{S}})}}\right), \quad (32)$$

$$F_{\gamma_1}(x) = 1 - \frac{2x^{n_{\mathsf{S}}/2}}{\Gamma(n_{\mathsf{S}})[\Omega_1\bar{\gamma}/(\mathcal{R}_c n_{\mathsf{S}})]^{n_{\mathsf{S}}/2}} \times \mathcal{K}_{n_{\mathsf{S}}}\left(2\sqrt{\frac{x}{\Omega_1\bar{\gamma}/(\mathcal{R}_c n_{\mathsf{S}})}}\right). \quad (33)$$

Moreover, the statistics of γ_2 can be obtained immediately from the PDF and CDF of $\|\boldsymbol{H}_{\mathrm{RD}}\|_{\mathrm{F}}^2$ given in (6) and (7), respectively. Our aim now is to calculate the MGF of $\gamma_{\mathsf{LA}}^{(\mathsf{up})}$. To do so, we differentiate (31) with respect to γ to obtain the PDF of $\gamma_{\mathsf{LA}}^{(\mathsf{up})}$ as

$$f_{\gamma_{\mathsf{LA}}^{(\mathsf{up})}}(\gamma|\gamma_2) = \frac{\epsilon c_2}{\gamma_2} f_{\gamma_1}\left(\frac{c_2\gamma}{\gamma_2}|\gamma_2\right) + \bar{\epsilon} f_{\gamma_1}(\gamma), \quad (34)$$

where $\epsilon = F_{\gamma_2}(c_2)$ can be deduced from (7) and $\bar{\epsilon} = 1-\epsilon$. As the MGF of $\gamma_{\mathsf{LA}}^{(\mathsf{up})}$ is the Laplace transform of its PDF, we have

$$\mathcal{M}_{\gamma_{\mathsf{LA}}^{(\mathsf{up})}}(s) = \epsilon\int_0^\infty \mathcal{M}_{\gamma_1}\left(\frac{s\gamma_2}{c_2}\right) f_{\gamma_2}(\gamma_2)\, d\gamma_2 + \bar{\epsilon}\mathcal{M}_{\gamma_1}(s), \quad (35)$$

where the first summand in (35) is obtained by exchanging the order of double integral, which is originated from the marginal PDF, with respect to the two variables γ and γ_2; and $\mathcal{M}_{\gamma_1}(s)$ is the MGF of γ_1 shown as follows:

$$\mathcal{M}_{\gamma_1}(s) = \frac{1}{\Omega_1\bar{\gamma}s/(\mathcal{R}_c n_{\mathsf{S}})}\Psi\left(1, 2-n_{\mathsf{S}}, \frac{1}{\Omega_1\bar{\gamma}s/(\mathcal{R}_c n_{\mathsf{S}})}\right), \quad (36)$$

where (36) follows from (32) and $\Psi(a,b;z)$ is the confluent hypergeometric function [18, Eq. (9.211.4)]. Since $n_{\mathsf{S}} \geq 2$, from (36) and using the fact that $\Psi(a,b;z) \overset{(\text{small } z)}{\approx} \frac{\Gamma(1-b)}{\Gamma(1+a-b)}$ if $b \leq 0$ [27], we get

$$\mathcal{M}_{\gamma_1}(s) \overset{(\text{large } \bar{\gamma})}{\approx} \frac{1}{(n_{\mathsf{S}}-1)\Omega_1\bar{\gamma}s/(\mathcal{R}_c n_{\mathsf{S}})}. \quad (37)$$

By substituting (37) and (6) into (35), the integral can be approximated as

$$\int_0^\infty \mathcal{M}_{\gamma_1}\left(\frac{s\gamma_2}{c_2}\right) f_{\gamma_2}(\gamma_2)\, d\gamma_2 \overset{(\text{large } \bar{\gamma})}{\approx} \frac{2\mathcal{R}_c n_{\mathsf{S}}}{\Omega_1 G_{\mathsf{LA}}^2(\Omega_2\bar{\gamma})^{(n_{\mathsf{R}}+n_{\mathsf{D}})/2}(n_{\mathsf{S}}-1)\Gamma(n_{\mathsf{R}})\Gamma(n_{\mathsf{D}})s} \times \int_0^\infty \gamma_2^{(n_{\mathsf{R}}+n_{\mathsf{D}})/2-2}\mathcal{K}_{n_{\mathsf{D}}-n_{\mathsf{R}}}\left(2\sqrt{\frac{\gamma_2}{\Omega_2\bar{\gamma}}}\right) d\gamma_2 = \frac{\mathcal{R}_c n_{\mathsf{S}}}{\Omega_1\Omega_2 G_{\mathsf{LA}}^2(n_{\mathsf{S}}-1)(n_{\mathsf{R}}-1)(n_{\mathsf{D}}-1)\bar{\gamma}s}, \quad (38)$$

where (38) is obtained by making use of [18, Eq. (6.561.16)]. Next, combining (37) and (38) with (35), the high SNR expression of the MGF of $\gamma_{\mathsf{LA}}^{(\mathsf{up})}$ can be rewritten as

$$\mathcal{M}_{\gamma_{\mathsf{LA}}^{(\mathsf{up})}}(s) = \left[\frac{\epsilon}{\Omega_2 G_{\mathsf{LA}}^2(n_{\mathsf{R}}-1)(n_{\mathsf{D}}-1)} + \bar{\epsilon}\right]\frac{\mathcal{R}_c n_{\mathsf{S}}}{\Omega_1(n_{\mathsf{S}}-1)\bar{\gamma}s}. \quad (39)$$

The asymptotic MGF of $\gamma_{\mathsf{LA}}^{(\mathsf{lo})}$ can be easily obtained from (39) by utilizing the fact that $\mathcal{M}_{\gamma_{\mathsf{LA}}^{(\mathsf{lo})}}(s) = \mathcal{M}_{\gamma_{\mathsf{LA}}^{(\mathsf{up})}}\left(\frac{1}{2}s\right)$. Hence, the asymptotic SEP can be shown in (13), which finalizes the proof.

APPENDIX C: PROOF OF THEOREM 3

We first consider for the case $n_{\mathsf{R}} \neq n_{\mathsf{D}}$. From (25) and (6), the asymptotic PDF of γ_2 can be given by

$$f_{\gamma_2}(\gamma_2) \overset{(\text{large } \bar{\gamma})}{\approx} \frac{\Gamma(|n_{\mathsf{D}} - n_{\mathsf{R}}|)}{\Gamma(n_{\mathsf{R}})\Gamma(n_{\mathsf{D}})} \frac{\gamma_2^{\min(n_{\mathsf{R}},n_{\mathsf{D}})-1}}{(\Omega_2\bar{\gamma})^{\min(n_{\mathsf{R}},n_{\mathsf{D}})}}. \tag{40}$$

Following the same approach as in [22][5], the SEP can be asymptotically obtained by the first non-zero high order derivative of $f_Z(z)$ as

$$P_{\mathrm{e}}^{(\mathsf{SRD})} \overset{(\text{large } \bar{\gamma})}{\approx} \frac{\prod_{i=1}^{d+1}(2i-1)}{(d+1)!}\left(\frac{\mathcal{R}_c n_{\mathsf{S}}}{2\mathsf{g}}\right)^{d+1} \frac{\partial^d}{\partial z^d} f_Z(0), \tag{41}$$

where $Z = \frac{\gamma_2\gamma_3}{\gamma_2+\gamma_3}$. Our main objective now is to study the behavior of $f_Z(z)$ in the high SNR regime. Let us write the PDF of Z as

$$f_Z(z) = f_{\gamma_2}(z) + \int_0^\infty \frac{\partial\left[F_{\gamma_3}\left(\frac{z^2}{x}+z\right) f_{\gamma_2}(z+x)\right]}{\partial z} dx. \tag{42}$$

Applying the Leibniz rule, the d-th order derivative of $f_Z(z)$ at zero value can be expressed as [18, Eq. 0.42]

$$\frac{\partial^d}{\partial z^d} f_Z(0) = \underbrace{\frac{\partial^d}{\partial z^n} f_{\gamma_2}(0)}_{\mathcal{I}_1} + \underbrace{\int_0^\infty \sum_{i=0}^{d+1} \binom{d+1}{i} \left.\frac{\partial^i F_{\gamma_3}\left(\frac{z^2}{x}+z\right)}{\partial z^i}\right|_{z=0} \left.\frac{\partial^{d+1-i} f_{\gamma_2}(z+x)}{\partial z^{d+1-i}}\right|_{z=0} dx}_{\mathcal{I}_2}. \tag{43}$$

The first summand $\mathcal{I}_1$ can be easily obtained from (40) as

$$\mathcal{I}_1 = \begin{cases} \frac{\Gamma(|n_{\mathsf{D}}-n_{\mathsf{R}}|)}{\Gamma(n_{\mathsf{R}})\Gamma(n_{\mathsf{D}})} \frac{\Gamma(\min(n_{\mathsf{R}},n_{\mathsf{D}}))}{(\Omega_2\bar{\gamma})^{\min(n_{\mathsf{R}},n_{\mathsf{D}})}} & \text{if } d = \min(n_{\mathsf{R}},n_{\mathsf{D}})-1, \\ 0 & \text{if } d < \min(n_{\mathsf{R}},n_{\mathsf{D}})-1. \end{cases} \tag{44}$$

To calculate the second summand $\mathcal{I}_2$, we use the i-th order derivative of the composite function [18, Eq. 0.430] which results in

$$\left.\frac{\partial^i F_{\gamma_3}\left(t=\frac{z^2}{x}+z\right)}{\partial z^i}\right|_{z=0} = \sum_{u=1}^{i}\sum_{v=0}^{u-1}\binom{u}{v}\frac{(-1)^v}{u!} t^v(0) \times \left.\frac{\partial^u F_{\gamma_3}(t)}{\partial t^u}\right|_{z=0} \left.\frac{\partial^i t^{u-v}}{\partial z^{u-v}}\right|_{z=0}. \tag{45}$$

It is observed that only $v=0$ makes $t^v(0) = \left.\left(\frac{z^2}{x}+z\right)^v\right|_{\gamma=0}$ be non-zero. From (16), the highest order of $F_{\gamma_3}(t)$ is $n_{\mathsf{S}}n_{\mathsf{R}}$ which allows us to select $u = n_{\mathsf{S}}n_{\mathsf{R}}$. Hence, (45) becomes

$$\left.\frac{\partial^i F_{\gamma_3}\left(t=\frac{z^2}{x}+z\right)}{\partial z^i}\right|_{z=0} = \frac{1}{\Gamma(n_{\mathsf{S}}n_{\mathsf{R}}+1)(\bar{\gamma})^{n_{\mathsf{S}}n_{\mathsf{R}}-1}} \left.\frac{\partial^i t^{n_{\mathsf{S}}n_{\mathsf{R}}}}{\partial z^{n_{\mathsf{S}}n_{\mathsf{R}}}}\right|_{z=0}. \tag{46}$$

It is obvious that $\mathcal{I}_2$ equals to zero when $d \leq \min(n_{\mathsf{R}},n_{\mathsf{D}})-1$. This is because with $i \leq d+1 \leq \min(n_{\mathsf{R}},n_{\mathsf{D}}) < n_{\mathsf{S}}n_{\mathsf{R}}$, (46) equals to zero. Hence, we will select $d = \min(n_{\mathsf{R}},n_{\mathsf{D}})-1$. By jointly considering the aforementioned results, we can obtain the asymptotic SEP as in (17).

Next we consider for the case $n_{\mathsf{R}} = n_{\mathsf{D}}$ by introducing the lower and upper bound of γ_{SA} as

$$\gamma_{\mathsf{SA}}^{(\mathsf{lo})} \triangleq \frac{1}{2\mathcal{R}_c n_{\mathsf{S}}}\min(\gamma_2,\gamma_3) \leq \gamma_{\mathsf{SA}} \leq \frac{1}{\mathcal{R}_c n_{\mathsf{S}}}\min(\gamma_2,\gamma_3) \triangleq \gamma_{\mathsf{SA}}^{(\mathsf{up})}. \tag{47}$$

As observed from (47), the bounds in this case involve two independent RVs as opposed to (12) which is related to two dependent RVs. Hence, it is important to note that although we use the lower and upper bounds as in Section III-B, the mathematical derivations will proceed differently. We are interested in deriving the MGF of $\gamma_{\mathsf{SA}}^{(\mathsf{up})}$ since the MGF of $\gamma_{\mathsf{SA}}^{(\mathsf{lo})}$ can be followed accordingly. Let us denote $T = \min(\gamma_2,\gamma_3)$. It is easy to see that as

$$\mathcal{M}_{\gamma_{\mathsf{SA}}^{(\mathsf{up})}}(s) = \mathcal{M}_{\gamma_2}\left(\frac{s}{\mathcal{R}_c n_{\mathsf{S}}}\right) + \mathcal{M}_{\gamma_3}\left(\frac{s}{\mathcal{R}_c n_{\mathsf{S}}}\right) - \int_0^\infty f_{\gamma_2}(t) F_{\gamma_3}(z) e^{-\frac{st}{\mathcal{R}_c n_{\mathsf{S}}}} dt - \int_0^\infty f_{\gamma_3}(t) F_{\gamma_2}(t) e^{-\frac{st}{\mathcal{R}_c n_{\mathsf{S}}}} dt. \tag{48}$$

To proceed, we substitute (7) into (48) and make use of the fact that γ_3 is the sum of $n_{\mathsf{S}}n_{\mathsf{R}}$ independent exponential variates. After several manipulations, the MGF of $\gamma_{\mathsf{SA}}^{(\mathsf{up})}$ can be re-expressed as

$$\mathcal{M}_{\gamma_{\mathsf{SA}}^{(\mathsf{up})}}(s) = \underbrace{\int_0^\infty \mathcal{A} f_{\gamma_2}(t) e^{-\frac{st}{\mathcal{R}_c n_{\mathsf{S}}}} dt}_{\mathcal{I}_3} + \underbrace{\int_0^\infty \mathcal{B} f_{\gamma_3}(t) e^{-\frac{st}{\mathcal{R}_c n_{\mathsf{S}}}} dt}_{\mathcal{I}_4}, \tag{49}$$

where $\mathcal{A}$ and $\mathcal{B}$ are, respectively, given by

$$\mathcal{A} = \sum_{k=0}^{n_{\mathsf{S}}n_{\mathsf{R}}-1}\left(\frac{t}{\Omega_1\bar{\gamma}}\right)^k \frac{e^{-\frac{t}{\Omega_1\bar{\gamma}}}}{k!},$$
$$\mathcal{B} = \sum_{k=0}^{n_{\mathsf{R}}-1}\frac{2}{\Gamma(n_{\mathsf{D}})k!}\left(\frac{t}{\Omega_2\bar{\gamma}}\right)^{(n_{\mathsf{D}}+k)/2} \mathcal{K}_{n_{\mathsf{D}}-k}\left(2\sqrt{\frac{t}{\Omega_2\bar{\gamma}}}\right). \tag{50}$$

When $n_{\mathsf{R}} = n_{\mathsf{D}}$, using (25) and (6), an asymptotic expression for the PDF of γ_2 can be obtained as

$$f_{\gamma_2}(t) \overset{(\text{large } \bar{\gamma})}{\approx} \frac{t^{n_{\mathsf{R}}-1}\ln\left(\frac{\Omega_2\bar{\gamma}}{t}\right)}{\Gamma(n_{\mathsf{R}})^2(\Omega_2\bar{\gamma})^{n_{\mathsf{R}}}}. \tag{51}$$

[5]Note that in different relay system contexts, the adopted asymptotic approach has been widely used in the existing literature to characterize the diversity and the array gains. See for example [28, Appendix] and [29].

Substituting (50) and (51) into (49) yields

$$\begin{aligned}\mathcal{I}_3 &\overset{(\text{large }\bar{\gamma})}{\approx} \sum_{k=0}^{n_{\mathsf{S}}n_{\mathsf{R}}-1} \frac{1}{\Gamma(n_{\mathsf{R}})^2\Omega_1^k\Omega_2^{n_{\mathsf{R}}}k!\bar{\gamma}^{n_{\mathsf{R}}+k}} \\ &\times \int_0^\infty t^{n_{\mathsf{R}}+k-1}e^{-(\frac{1}{\Omega_1\bar{\gamma}}+\frac{s}{\mathcal{R}_c n_{\mathsf{S}}})t}\ln\left(\frac{\Omega_2\bar{\gamma}}{t}\right)dt, \\ &\overset{(\text{large }\bar{\gamma})}{\approx} \sum_{k=0}^{n_{\mathsf{S}}n_{\mathsf{R}}-1} \frac{\Gamma(n_{\mathsf{R}}+k)\left[\ln\left(\frac{\Omega_2\bar{\gamma}s}{\mathcal{R}_c n_{\mathsf{S}}}\right)-\psi(n_{\mathsf{R}}+k)\right]}{\Gamma(n_{\mathsf{R}})^2\Omega_1^k\Omega_2^{n_{\mathsf{R}}}k!} \\ &\times \left(\frac{\mathcal{R}_c n_{\mathsf{S}}}{\bar{\gamma}s}\right)^{n_{\mathsf{R}}+k}, \end{aligned} \tag{52}$$

where (52) is obtained by using $\frac{1}{\Omega_1\bar{\gamma}} \overset{(\text{large }\bar{\gamma})}{\ll} \frac{1}{\mathcal{R}_c n_{\mathsf{S}}}$ and [18, Eq. (4.352.1)]. Similarly, we get the following approximation for $\mathcal{I}_4$:

$$\mathcal{I}_4 \overset{(\text{large }\bar{\gamma})}{\approx} \sum_{k=0}^{n_{\mathsf{R}}-1} \frac{\Gamma(n_{\mathsf{R}}-k)\Gamma(n_{\mathsf{S}}n_{\mathsf{R}}+k)}{\Gamma(n_{\mathsf{R}})\Gamma(n_{\mathsf{S}}n_{\mathsf{R}})\Omega_2^k\Omega_1^{n_{\mathsf{S}}n_{\mathsf{R}}}k!}\left(\frac{\mathcal{R}_c n_{\mathsf{S}}}{\bar{\gamma}s}\right)^{n_{\mathsf{S}}n_{\mathsf{R}}+k}. \tag{53}$$

Since $\mathcal{I}_3$ and $\mathcal{I}_4$ are proportional to $\left(\frac{1}{\bar{\gamma}}\right)^{n_{\mathsf{R}}+k}$ and $\left(\frac{1}{\bar{\gamma}}\right)^{n_{\mathsf{S}}n_{\mathsf{R}}+k}$ with k being an integer, respectively, $\mathcal{I}_4$ can be neglected as compared to $\mathcal{I}_3$. Then by selecting the index $k=0$ (higher values of k can be omitted) for $\mathcal{I}_3$, the asymptotic MGF of $\gamma_{\mathsf{SA}}^{(\mathsf{up})}$ is given by

$$\mathcal{M}_{\gamma_{\mathsf{SA}}^{(\mathsf{up})}}(s) \overset{(\text{large }\bar{\gamma})}{\approx} \frac{\ln\left(\frac{\Omega_2\bar{\gamma}s}{\mathcal{R}_c n_{\mathsf{S}}}\right)-\psi(n_{\mathsf{R}})}{\Gamma(n_{\mathsf{R}})\Omega_2^{n_{\mathsf{R}}}}\left(\frac{\mathcal{R}_c n_{\mathsf{S}}}{\bar{\gamma}s}\right)^{n_{\mathsf{R}}}. \tag{54}$$

Using (54), the SEP behavior in the high SNR regime pertaining to the case of $n_{\mathsf{R}} = n_{\mathsf{D}}$ can be given by (18), which concludes our proof.

Appendix D: Proof of Theorem 4

When $n_{\mathsf{R}} > n_{\mathsf{D}}$, by following the same approach as in Section III-C, we can easily obtain (21). For the case $n_{\mathsf{R}} < n_{\mathsf{D}}$, we can obtain $\mathcal{I}_1$ given in (43) as

$$\mathcal{I}_1 = \begin{cases} \frac{\Gamma(n_{\mathsf{D}}-n_{\mathsf{R}})}{\Gamma(n_{\mathsf{D}})(\Omega_2\bar{\gamma})^{n_{\mathsf{R}}}} & \text{if } d = n_{\mathsf{R}}-1, \\ 0 & \text{if } d < n_{\mathsf{R}}-1. \end{cases} \tag{55}$$

In Section III-C, $\mathcal{I}_2$ given in (43) is zero. In contrast, $\mathcal{I}_2$ now becomes non-zero and the index i can be selected as $i = d+1 = n_{\mathsf{R}}$, which then allows us to rewrite the right-hand-side of (45) as $\frac{\Gamma(n_{\mathsf{S}}-n_{\mathsf{R}})}{\Gamma(n_{\mathsf{S}})(\Omega_1\bar{\gamma})^{n_{\mathsf{R}}}}$. In addition, the term $\left.\frac{\partial^{d+1-i}f_{\gamma_2}(z+x)}{\partial z^{d+1-i}}\right|_{z=0}$ of $\mathcal{I}_2$ given in (43) now becomes $f_{\gamma_2}(x)$ and is given by $\mathcal{I}_2 = \frac{\Gamma(n_{\mathsf{S}}-n_{\mathsf{R}})}{\Gamma(n_{\mathsf{S}})(\Omega_1\bar{\gamma})^{n_{\mathsf{R}}}}$. Utilizing this result and pulling (55) together with (43) and (41), the asymptotic SEP is expressed as (22). The derivation for the case $n_{\mathsf{R}} = n_{\mathsf{D}}$ follows the same pattern as in Section III-C and therefore is omitted for brevity. Specifically, the result of $\mathcal{I}_3$ can be shown as

$$\mathcal{I}_3 \overset{(\text{large }\bar{\gamma})}{\approx} \frac{\left[\ln\left(\frac{\Omega_1\bar{\gamma}s}{\mathcal{R}_c n_{\mathsf{S}}}\right)-\psi(n_{\mathsf{R}})\right]}{\Gamma(n_{\mathsf{R}})\Omega_2^{n_{\mathsf{R}}}}\left(\frac{\mathcal{R}_c n_{\mathsf{S}}}{\bar{\gamma}s}\right)^{n_{\mathsf{R}}}. \tag{56}$$

In contrast to the derivation in Section III-C, $\mathcal{I}_4$ can not be neglected. In fact, it is comparable with $\mathcal{I}_3$ and can be expressed as

$$\mathcal{I}_4 \overset{(\text{large }\bar{\gamma})}{\approx} \frac{\Gamma(n_{\mathsf{S}}-n_{\mathsf{R}})}{\Gamma(n_{\mathsf{R}})\Omega_1^{n_{\mathsf{R}}}}\left(\frac{\mathcal{R}_c n_{\mathsf{S}}}{\bar{\gamma}s}\right)^{n_{\mathsf{R}}}. \tag{57}$$

which then allows us to obtain (23), which finally completes the proof.

References

[1] D. Gesbert, M. Shafi, D. shan Shiu, P. J. Smith, and A. Naguib, "From theory to practice: an overview of MIMO space-time coded wireless systems," *IEEE J. Sel. Areas Commun.*, vol. 21, no. 3, pp. 281–302, Apr. 2003.

[2] S. Loyka and A. Kouki, "On MIMO channel capacity, correlations, and keyholes: analysis of degenerate channels," *IEEE Trans. Commun.*, vol. 50, no. 12, pp. 1886–1888, Dec. 2002.

[3] P. Almers, F. Tufvesson, and A. F. Molisch, "Keyhole effects in MIMO wireless channels-measurements and theory," *IEEE Trans. Wireless Commun.*, vol. 5, no. 12, pp. 3596–3604, Dec. 2006.

[4] H. Shin and J. H. Lee, "Performance analysis of space–time block codes over keyhole Nakagami-m fading channels," *IEEE Trans. Veh. Technol.*, vol. 53, no. 2, pp. 351–362, Mar. 2004.

[5] Y. Fan and J. Thompson, "MIMO configurations for relay channels: theory and practice," *IEEE Trans. Wireless Commun.*, vol. 6, no. 5, pp. 1774–1785, May 2007.

[6] H. S. Muhaidat, M. Uysal, and R. Adve, "Pilot-symbol-assisted detection scheme for distributed orthogonal space–time block coding," *IEEE Trans. Wireless Commun.*, vol. 8, no. 3, pp. 1057–1061, Mar. 2009.

[7] O. Souihli and T. Ohtsuki, "Cooperative diversity can mitigate keyhole effects in wireless MIMO systems," in *Proc. 2009 IEEE GLOBECOM*, pp. 1–6.

[8] ——, "The MIMO relay channel in the presence of keyhole effects," in *Proc. 2010 IEEE ICC*.

[9] T. Q. Duong, H. A. Suraweera, T. A. Tsiftsis, H.-J. Zepernick, and A. Nallanathan, "OSTBC transmission in MIMO AF relay systems with keyhole and spatial correlation effects," in *Proc. 2011 IEEE ICC*, pp. 1–6.

[10] T. Q. Duong, H. Shin, and E.-K. Hong, "Effect of line-of-sight on dual-hop nonregenerative relay wireless communications," in *Proc. 2007 IEEE VTC – Fall*, pp. 571–575.

[11] P. Dharmawansa, M. R. McKay, and R. K. Mallik, "Analytical performance of amplify-and-forward MIMO relaying with orthogonal space–time block codes," *IEEE Trans. Commun.*, vol. 58, no. 7, pp. 2147–2158, July 2010.

[12] X. Li, T. Luo, G. Yue, and C. Yin, "A squaring method to simplify the decoding of orthogonal space-time block codes," *IEEE Trans. Commun.*, vol. 49, no. 10, pp. 1700–1703, Oct. 2001.

[13] I.-H. Lee and D. Kim, "End-to-end BER analysis for dual-hop OSTBC transmissions over Rayleigh fading channels," *IEEE Trans. Commun.*, vol. 56, no. 3, pp. 347–351, Mar. 2008.

[14] S. Chen, W. Wang, and X. Zhang, "Performance analysis of OSTBC transmission in amplify-and-forward cooperative relay networks," *IEEE Trans. Veh. Technol.*, vol. 59, no. 1, pp. 105–113, Jan. 2010.

[15] L. Yang and Q. T. Zhang, "Performance analysis of MIMO relay wireless networks with orthogonal STBC," *IEEE Trans. Veh. Technol.*, vol. 59, no. 7, pp. 3668–3674, Sep. 2010.

[16] H. İlhan, M. Uysal, and İ. Altunbas, "Cooperative diversity for intervehicular communication performance analysis and optimization," *IEEE Trans. Veh. Technol.*, vol. 38, no. 3, pp. 1218–1228, Mar. 2009.

[17] F. Gong, J. Ge, and N. Zhang, "SER analysis of the mobile-relay-based M2M communication over double Nakagami-m fading channels," *IEEE Commun. Lett.*, vol. 15, no. 1, pp. 34–36, Jan. 2011.

[18] I. S. Gradshteyn and I. M. Ryzhik, *Table of Integrals, Series, and Products*, 6th edition. Academic, 2000.

[19] V. Tarokh, H. Jafarkhani, and A. R. Calderbank, "Space–time block codes from orthogonal designs," *IEEE Trans. Inf. Theory*, vol. 45, no. 5, pp. 1456–1467, July 1999.

[20] O. Tirkkonen and A. Hottinen, "Square-matrix embeddable space–time block codes for complex signal constellations," *IEEE Trans. Inf. Theory*, vol. 48, no. 2, pp. 384–395, Feb. 2002.

[21] D. Chizhik, G. J. Foschini, M. J. Gans, and R. A. Valenzuela, "Keyholes, correlations, and capacities of multielement transmit and receive antennas," *IEEE Trans. Wireless Commun.*, vol. 1, no. 2, pp. 361–368, Apr. 2002.

[22] A. Ribeiro, X. Cai, and G. B. Giannakis, "Symbol error probabilities for general cooperative links," *IEEE Trans. Wireless Commun.*, vol. 4, no. 3, pp. 1264–1273, May 2005.
[23] Y. Jing and B. Hassibi, "Distributed space-time coding in wireless relay networks," *IEEE Trans. Wireless Commun.*, vol. 5, no. 12, pp. 3524–3536, Dec. 2006.
[24] Y. Jing and H. Jafarkhani, "Using orthogonal and quasi-orthogonal designs in wireless relay networks," *IEEE Trans. Inf. Theory*, vol. 53, no. 11, pp. 4106–4118, Nov. 2007.
[25] M. Abramowitz and I. A. Stegun, *Handbook of Mathematical Functions*. Dover Publications Inc., 1974.
[26] A. P. Prudnikov, Y. A. Brychkov, and O. I. Marichev, *Integrals and Series, Vol. 1*. Gordon and Breach Science, 1986.
[27] M. Abramowitz and I. A. Stegun, *Handbook of Mathematical Functions with Formulas, Graphs, and Mathematical Tables*. U.S. Dept. of Commerce, 1970.
[28] Z. Fang, L. Li, and Z. Wang, "Asymptotic performance analysis of multihop relayed transmissions over Nakagami-m fading channel," *IEICE Trans. Commun.*, vol. E91-B, no. 12, pp. 4081–4084, Dec. 2008.
[29] F. Xu, F. C. M. Lau, and D.-W.Yue, "Diversity order for amplify-and-forward dual-hop systems with fixed-gain relay under Nakagami fading channels," *IEEE Trans. Wireless Commun.*, vol. 9, no. 1, pp. 92–98, Jan. 2010.

Trung Q. Duong (S'05) was born in HoiAn town, Quang Nam province, Vietnam, in 1979. He received the B.S. degree in electrical engineering from Ho Chi Minh City University of Technology, Vietnam in 2002, and the M.Sc. degree in computer engineering from Kyung Hee University, South Korea, in 2005. In April 2004, he joined the faculty of electrical engineering of Ho Chi Minh City University of Transport, Vietnam. He was a recipient of the Korean Government IT Scholarship Program for International Graduate Students from 2003 to 2007. He was awarded the Best Paper Award of IEEE Student Paper Contest - IEEE Seoul Section in December 2006 and was listed in the finalist for the best paper award at the IEEE Radio and Wireless Symposium, San Diego, U.S.A. in 2009.

Mr. Duong has been acting as a frequent reviewer for numerous journals/conferences and a TPC member for many conferences including ICC, WCNC, VTC, PIMRC. He has been a TPC co-chair of the International Conference on Computing, Managements, and Telecommunications 2013 (ComManTel2013). He has been working as a visiting scholar at Polytechnic Institute of New York University from December 2009 to January 2010 and Singapore University of Technology and Design from July 2012 to August 2012. In December 2007, he joined the Radio Communication Group, Blekinge Institute of Technology, Sweden as a research staff working toward his Ph.D. degree in radio communications. His current research interests include cross-layer design, cooperative communications, and cognitive radio networks.

Himal A. Suraweera (S'04, M'07) received the B.Sc. degree (first class honors) in electrical and electronics engineering Peradeniya University, Peradeniya, Sri Lanka, in 2001 and the Ph.D. degree from Monash University, Melbourne, Australia, in 2007. He was also awarded the 2007 Mollie Holman Doctoral and 2007 Kenneth Hunt Medals for his doctoral thesis upon graduating from Monash University. From 2001 to 2002, he was with the Department of Electrical and Electronics Engineering, Peradeniya University, as an Instructor. From October 2006 to January 2007 he was at Monash University as a Research Associate. From February 2007 to June 2009, he was at the center for Telecommunications and Microelectronics, Victoria University, Melbourne, Australia as a Research Fellow. From July 2009 to January 2011, he was with the Department of Electrical and Computer Engineering, National University of Singapore, Singapore as a Research Fellow. He is now a Research Fellow at the Singapore University of Technology and Design, Singapore. His main research interests include relay networks, cognitive radio, MIMO, wireless security and Green communications.

Dr. Suraweera is an associate Editor of the IEEE COMMUNICATIONS LETTERS. He received an IEEE COMMUNICATIONS LETTERS exemplary reviewer certificate in 2009 and an IEEE Communications Society Asia-Pacific Outstanding Young Researcher Award in 2011. He was a recipient of an International Postgraduate Research Scholarship from the Australian Commonwealth during 2003-2006.

Theodoros A. Tsiftsis (S'02-M'04-SM'10) was born in Lamia, Greece, in November 1970. He received the degree in Physics from the Aristotle University of Thessaloniki, Greece, in 1993, and the M.Sc. degree in Digital Systems Engineering from the Heriot-Watt University, Edinburgh, Scotland, U.K., in 1995. Also, he received the M.Sc. degree in Decision Sciences from the Athens University of Economics and Business, Greece, in 2000 and the Ph.D. degree in Electrical Engineering from the University of Patras, Greece, in 2006. He is currently an Assistant Professor in the Department of Electrical Engineering at Technological Educational Institute of Lamia, Greece.

His major research interests include relay assisted and cooperative communications,wireless communications over fading channels, wireless communications theory and optical wireless communications. He has published and presented more than 50 technical papers in scientific journals and international conferences.

Dr. Tsiftsis acts as reviewer for several international journals and he is member of the Editorial Boards of IEEE TRANSACTIONS ON VEHICULAR TECHNOLOGY, IEEE COMMUNICATIONS LETTERS and *IET Communications*.

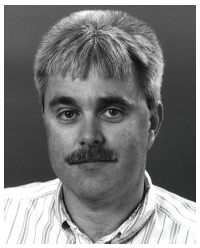

Hans-Jürgen Zepernick (M'94-SM'11) received the Dipl.-Ing. degree from the University of Siegen in 1987 and the Dr.-Ing. degree from the University of Hagen in 1994. From 1987 to 1989, he was with Siemens AG, Germany. He is currently a Professor of radio communications at the Blekinge Institute of Technology, Sweden. Prior to this appointment, he held the positions of Professor of wireless communications at Curtin University of Technology; Deputy Director of the Australian Telecommunications Research Institute; and Associate Director of the Australian Telecommunications Cooperative Research Centre. His research interests include cooperative communications, cognitive radio networks, mobile multimedia, and perceptual quality assessment.

Arumugam Nallanathan (S'97-M'00-SM'05) is the Head of Graduate Studies in the School of Natural and Mathematical Sciences and a Reader in Communications at King's College London, London, U.K. From August 2000 to December 2007, he was an Assistant Professor in the Department of Electrical and Computer Engineering at the National University of Singapore, Singapore. His research interests include smart grid, cognitive radio, and relay networks. He has authored nearly 200 journal and conference papers. He is an Editor for IEEE TRANSACTIONS ON COMMUNICATIONS, IEEE TRANSACTIONS ON VEHICULAR TECHNOLOGY, IEEE WIRELESS COMMUNICATIONS LETTERS, and IEEE SIGNAL PROCESSING LETTERS. He served as an Editor for IEEE TRANSACTIONS ON WIRELESS COMMUNICATIONS (2006-2011) and as a Guest Editor for the *EURASIP Journal of Wireless Communications and Networking: Special Issue on UWB Communication Systems-Technology and Applications*. He served as the General Track Chair for the Spring 2008 IEEE Vehicular Technology Conference (VTC'2008) and Co-Chair for the 2008 IEEE Global Communications Conference (GLOBECOM'2008) Signal Processing for Communications Symposium, 2009 IEEE International Conference on Communications (ICC'2009) Wireless Communications Symposium, 2011 IEEE Global Communications Conference (GLOBECOM'2011) Signal Processing for Communications Symposium and the 2012 IEEE International Conference on Communications (ICC'2012) Signal Processing for Communications Symposium. He also served as the Technical Program Co-Chair for the 2011 IEEE International Conference on Ultra-Wideband (ICUWB'2011). He currently serves as the Co-Chair for the 2013 IEEE Global Communications Conference (GLOBECOM'2013) Communications Theory Symposium. He is the Vice-Chair for the Signal Processing for Communication Electronics Technical Committee of the IEEE Communications Society. He was a co-recipient of the Best Paper Award presented at the 2007 IEEE International Conference on Ultra-Wideband.